ADDIS ABABA UNIVERSITY

SCHOOL OF GRADUATE STUDIES

COLLAGE OF NATURAL SCIENCE

SCHOOL OF EARTH AND PLANETARY SCIENCE

DEPARTMENT OF EARTH SCIENCE

INTEGRATED GEOPHYSICAL INVESTIGATIONS FOR GOLD EXPLORATION IN DEMBI DOLO ZONE, WESTERN ETHIOPIA

BY

FANTAHUN GEBRIE TESHOME

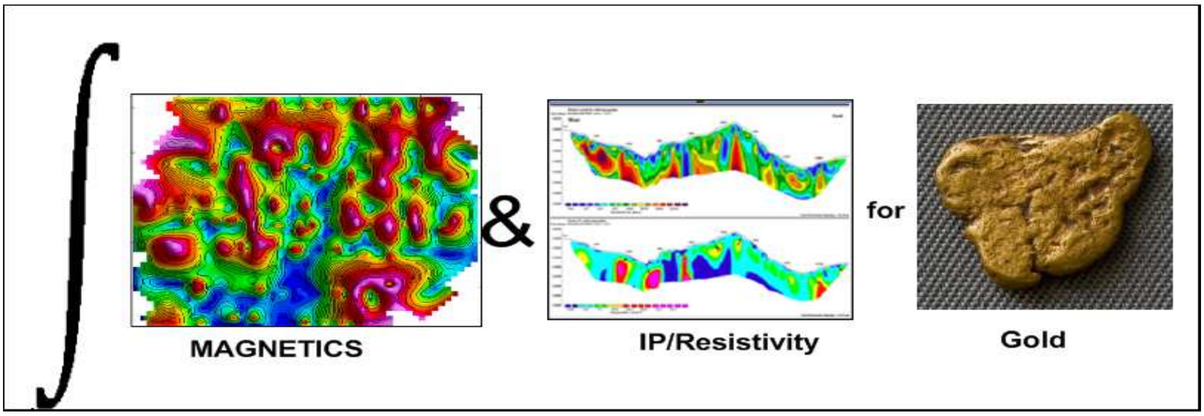

A Thesis Submitted to the School of Graduate Studies of Addis Ababa University in Partial Fulfillment of the Requirement for the Degree of Masters of Science in Earth Science (Exploration Geophysics)

ADDIS ABABA

November 2011

Addis Ababa University

School of Graduate Studies

Collage of Natural Science

School of Earth and Planetary Science

Department of Earth Science

Integrated Geophysical Investigations for Gold in Dembi Dolo Zone, Western Ethiopia

By

Fantahun Gebrie Teshome

Approved by board of examiners:

Dr. Tigistu Haile signature_______________
(Chairman, Department of Geophysics)

Dr. Shimeles Fisseha signature_______________
Advisor

Professor Solomon Tadesse signature_______________
Co-advisor

Dr. Tilahun Mammo signature_______________
Internal Examiner

Dr. Worash Getaneh signature_______________
External Examine

November 2011

ACKNOWLEDGMENT

First of all, I would like to thank the almighty God for the many blessings.

I have no words to thank my advisor Dr. Shimeles Fisseha for his decisive guidance throughout this thesis work. The constructive suggestions he gave me were important to accomplish the work and this final manuscript. Moreover, I would like to thank him for arranging financial supports during the fieldwork and, office space equipped with computational facilities for processing geophysical data. Your support in suggesting valuable reference books and in sharing your field and research experiences contributed greatly. Thank you and God bless you.

I would like to express my heartfelt thanks to my co-advisor, Prof. Solomon Tadesse for his support and comment for the success of this thesis.

I want to acknowledge Dr. Tigistu Haile for his help in collecting geophysical data and for his sharing his instrument and experience during the fieldwork.

I am so grateful to EL-Mining Plc. where I got the geophysical data, geochemical and geological reports of the study area and Institution of Geophysics, Space Science and Astronomy (IGSSA) for giving me an office with computer facilities to carry out geophysical data processing and preparation of this manuscript.

I extend my acknowledgement to all my friends Yahya Ali., Tagel Asefa., Bereket G., Haylemariam S. for their help in learning the geophysical data processing software and for suggesting other supporting ideas.

Finally yet importantly, my sincere thank goes to my wife, W/t Firehiwot Abate for her unreserved encouragement patience, and help which was so vital to accomplish this work.

TABLE OF CONTENTS

ACKNOWLEDGMENT ii
TABLE OF CONTENTS iii
LIST OF FIGURES vi
ACRONYMS vi
ABSTRACT viii
CHAPTER ONE 1
Introduction 1
1.1 General 1
1.1.1 Geophysical Methods for Mineral Exploration 2
1.2 THE STUDY AREA 3
1.2.1 Location and Accessibility of the Area 3
1.2.2 Climate and Vegetation 4
1.3 Previous Work in the Study Area 6
1.4 Problem Definition 6
1.5 Objectives of the Present Work 7
1.6 Methodology 8
CHAPTER TWO 9
GEOLOGICAL BACKGROUND 9
2.1 Regional Geological Setting 9
2.2 Geological Setting of the Study Area 13
2.2.1 Gneissic Rocks 13
2.2.2 Metasedimentary-Metavolcanic Assemblages 13

2.3 Structural Setting of the Study Area 15

2.4 Metamorphism and Alteration 17

2.5 Prospecting For Gold Deposits 17

2.6 Indications of Gold Mineralization in the study area 18

CHAPTER THREE 21

GEOPHYSICAL DATA ACQUISITION AND PROCESSING 21

3 General 21

3.1 The Electrical IP/Resistivity Survey 21

3.1.1 Instrumentation 21

3.1.2 IP/Resistivity Field Procedures 22

3.1.3 IP/Resistivity Data Processing and Presentation 22

3.2 The Magnetic Survey 24

3.2.1 Instrumentation 24

3.2.2 Magnetic Data Acquisition 24

3.2.3 Magnetic Data Processing 25

3.2.4 Magnetic Data Presentation 26

CHAPTER FOUR 27

DISCUSSION OF RESULTS AND INTERPRETATION 27

4. Results and Interpretations of Different Anomaly Maps 27

4.1 Total Observed Magnetic Field Intensity Map 27

4.2 Analytical signal map 28

4.2.1 First Vertical Derivative Map of Analytic signal 30

4.2.2 Tilt Derivative of the Analytic Signal Map 31

4.3 IP/Resistivity result discussion and interpretations 34

4.3.1 IP/Resistivity Inverse Model Section 800S 34

4.3.2 IP/Resistivity Inverse Model Section 600S 37

4.3.3 IP/Resistivity Inverse Model Section 400S 39

4.3.4 IP/Resistivity Inverse Model Section 200N 41

4.3.5 IP/Resistivity Inverse Model Section 800N 43

4.3.6 IP/Resistivity Inverse model section 1200N 45

4.4 Resistivity and Chargeability Sliced Stacked Depth Maps 47

CHAPTER FIVE 50

CONCLUTION AND RECOMMENDATION 50

5.1 CONCLUSIONS 50

5.2 RECOMMENDATIONS 51

Appendix I 53

Basic principles of (DC) Resistivity method 53

APPENDIX II 61

Induced Polarization Method 61

APPENDIX III 64

Magnetic Survey Method 64

REFERENCES 72

LIST OF FIGURES

Figure 1.1 Location map of the study area in the project Area. 5

Figure 2.1 Geological map of the project area showing major structures and the location of the detail study area (EL-Mining annual report, May 2010). 10

Figure 2.2 The project area`s four blocks and the location of the follow up areas (EL-Mining annual report, May 2010). 12

Figure 2.3 Geological map and cross section of the study area (EL-Mining annual report, May 2010). 16

Figure 2.4 Geochemical map of the study area and IP/Resistivity lines (EL-Mining annual report, March 2011) 20

Figure 3.1 Magnetic profile and IP/Resistivity lines on geological map of the study area. 21

Figure 4.1 Total observed ground magnetic field intensity map 27

Figure 4.2 Analytic signals map.. 29

Figure 4.3 First vertical derivative of the analytic signal.. 31

Figure 4.4 Tilt derivative of the analytic signal.. 32

Figure 4.5 Inverse resistivity and chargeability model section of 800S................. 36

Figure 4.6 Inverse model resistivity and chargeability section 600S...................... 38

Figure 4.7 Inverse model resistivity and chargeability section of 400S................. 40

Figure 4.8 Inverse model resistivity and chargeability section of 200N 42

Figure 4.9 Inverse resistivity and chargeability section of 800N 44

Figure 4.10 Inverse model resistivity and chargeability section of 1200N 46

Figure 4.11 Stacked interpreted resistivity at different depth values 48

Figure 4.12 Stacked interpreted chargeability at different depths......................... 49

ACRONYMS

ANS= Arabian Nubian Shield

AS= Analytic Signal

DGRF=Definitive Geomagnetic Reference Field

E-W= East –West

ENE-WSW=East North East-West South West

GPS=Global Positioning System

GSE= Geological Survey of Ethiopia

IGRF=International Geomagnetic Reference Field

IP/Res= Induced Polarization/Resistivity

Mag= Magnetics

NOAA= National Oceanic and Atmospheric Administration

N-S= North-south

NNE-SSW= North North East- South South West

NNW-SSE= North North West- South South East

NW-SE= North West-South East

RMSE=Root Mean Square Error

TDR=Tilt Derivatives

TMFI=Total Magnetic Field Intensity

WNW-ESE= West North West-East South East

WES= Western Ethiopian Shield

2D= Two Dimensional

200N, 800N, 1200N=200, 800, 1200 (North)

800S, 600S, 400S=800,600,400 (South)

ABSTRACT

This manuscript presents a Masters degree thesis dealing with an integrated, IP/Resistivity and magnetic, surveys conducted as part of a systematic exploration program to map the subsurface litho-structural features favourable for gold mineralization in Gute Soyoma area, Dembi-Dolo zone, of western Ethiopia. The geophysical surveys particularly aim at mapping the subsurface signatures of rock units and structural controls responsible for the observed high gold values seen in a systematic geochemical survey over selected targets.

Geologically, the study area is located in the western Ethiopia shield and covered with basement rocks hosting economic metallic mineral deposits. It consists of gneissic rocks and metasedimentary-metavolcanics assemblages (amphibolite to greenschist facies). These rock assemblages host gold and other base metal mineralizations.

Qualitative interpretation of the total field magnetic data along eight profiles showed the presence of magnetic minerals and possible shear related structures, which are litho-structural indications of gold mineralization. On the other hand, appraisal of six traverse lines of IP/Resistivity data revealed that along most of the survey lines, over the regions of high gold showings, high IP amplitudes (>25mV/V), over a background of 1 – 5mV/V, were detected and very often, spatially associated to zones very high resistivity (in excess of 2000Ωm). These are interpreted to arise from sulphide minerals in silicified zones, which are closely associated to the main structural features such as shearing.

The current results of the integrated methods of IP/Resistivity and magnetic have showed good correlations, reduced the ambiguity inherent of the geophysical data interpretations, and highlights the sulphide minerals are disseminated type and hosted by intuitively silicified rocks. These prominent geophysical anomalous zones attributed to the mineralized zone have been shown to be open to the eastern and southern border of the current detail area. Therefore, continuation along these directions is highly recommended.

CHAPTER ONE

Introduction

1.1 General

Ethiopia is endowed with various types of metallic minerals such as gold, platinum, copper, lead, zinc, tantalite-dolomite, manganese, molybdenum etc. This mineral potential, coupled with the attractive and conducive investment environment, definitely magnifies the possibility of discovering economic deposits and it is essential of knowing the geology of the country. In general, the geology of Ethiopia ranges from oldest (Precambrian) to recent volcanic and sedimentary formation.

The oldest (Precambrian) rocks host most of the economic metallic mineral deposits that include primary and secondary enriched (placer) gold, platinum, platinum group elements (PGE), nickel, base metals (like copper, lead and Zinc), industrial minerals (like phosphate, iron ore),gemstones (like ruby, emerald, sapphire, garnet, etc) and also decorative and dimension stones such as marble, granite and other coloured stones.

Secondary enriched (placer) gold has been mined traditionally (artisinaly) for years back to biblical times in the history of Ethiopia. The gold being mined by artisanal miners nationwide is estimated at more than 3.5t/y in the Adola greenstone belt and southern greenstone belt (MMEFDRE) scribd.com).

However, in the search of mineral deposits, it is impossible to examine in detail every square km of an area, for example drilling. This would be too expensive, time consuming and in most cases pointless. An area where the required mineral resources can be expected to occur is therefore delimited using prospecting (geological, geochemical and geophysical) criteria, that is, geological features that directly or indirectly suggest the presence of a given deposit. As surface out cropping deposit become less common, the scope of surface geological and geochemical investigations have become less effective. Therefore, the main objective of this study is to identify mineral potential zones by incorporating geophysical methods for exploring mineral resources and minimize the risk of inappropriate areas of drilling borehole. Thus, geophysical methods contribute most at the surface in exploration.

1.1.1 Geophysical Methods for Mineral Exploration

The science of geophysics applies the principles of physics to the study of the Earth. Geophysical investigations of the interior of the Earth involve taking measurements at or near the Earth's surface that are influenced by the internal distribution of physical properties. Analysis of these measurements can reveal how the physical properties of the Earth's interior vary vertically and laterally.

Geophysical surveying, although sometimes prone to major ambiguities or uncertainties of interpretation, provides a relatively rapid and cost-effective means of deriving a really distributed information on subsurface geology. In the exploration for subsurface resources, the methods are capable of detecting and delineating local features of potential interest that could not be discovered by any realistic drilling programme. Geophysical surveying does not dispense with the need for drilling but, properly applied, it can optimize exploration programmes by maximizing the rate of ground coverage and minimizing the drilling requirement.

Geophysical techniques have being used in mineral prospecting for the past 300 years, beginning in Sweden around 1640 with the use of magnetic compasses in exploring for iron ore(zonge.com).

The most widely used geophysical techniques in mineral exploration works include the magnetic, gravity, electrical, and electromagnetic. These techniques used to apply the investigation of the subsurface information. Practically, the selection of the right geophysical method as well as the condition of application depends on a great many considerations. Some of the more important of which may be, the particular purpose of the survey, budget constraints, general geology of the study area information already available, local geology (probable type of structure, etc), depth of investigation required to study, terrain conditions, and others.

The existing topography, geological and mineralogical information is considered to decide whether geophysical methods should be used in the area at all and, if they are used, which of them would be the most suitable (Parasins, 1975). Sometimes, the desired mineralized target may have a physical property (parameter) that persist direct detection. For instance, Lead/Zinc deposits (galena/sphalerite) have large densities that may be detected directly by a gravity survey. However, the magnetic method is very suitable for locating buried magnetite ore bodies because of their high magnetic susceptibility.

Electrical methods have broad application to mineral they may be used to identify sulfide minerals and can be used to identify structures and lithologies. Resistivity measurements followed in the 1800's in the search for base metals, and by 1912, Conrad Schlumberger had patented the induced polarization (IP) method, and had used the technique for finding economic sulphide deposits (zonge.com).

Geophysical methods are often used in combination. At the interpretation stage, ambiguity arising from the results of one survey method may often be removed by consideration of results from a second survey method. Therefore, integrated approach in this specific study helps to reduce the uncertainty innate in the geophysical data combine with geochemical and geological knowledge of the study area.

1.2 THE STUDY AREA

1.2.1 Location and Accessibility of the Area

The study area (Gute Soyoma) is specifically found in Oromia National Regional State, Kelem-Wollega (West Wollega) and Illibabur Zones, in the southwestern part of Ethiopia. The area lies between the UTM coordinates: 938684-940971 Northing and ; 711270-713828 Easting and covers a total area of about 4.48 Sq. Km. falls in Hawa Welel, Seyo and Gawo Dale Weredas under Kelem-Wolega Zone. The present research has covers only 4.84sq.km from the total 1680 sq.km area of the license area. The land distance to the area is 665 km west of Addis Ababa, the area accessed by via two main roads that connect the capital, Addis Ababa, and Gambela town. There are two choices to reach to the area. One choice from Addis-Jimma-Gambela-Dembidolo, which is 865km land distance. The second choice is through Addis-Nekemt-Gimbi-Dembidolo, which is 665km.

The principal administrative centers, relatively close to the study area, are Dembidolo, the Kelem zone administrative town and Mojo, Rob-Gebeya and Mechara are smaller towns within Kelem zone. The exploration study area can have various feeder roads from these towns.

The area under study is in the shoulder of the Western highlands of Ethiopia and the low elevation noted within river cuts measuring up to 1270ma.s.l. Altitudes of ridges having elevations of 1480m above sea level are also recorded within the study area.

1.2.2 Climate and Vegetation

The climate of the license area generally categorized as moderately humid to arid tropical, with annual precipitation of 880mm. It has two main rainy seasons from September to October and from March to May. The climatic condition favors for the plantation of false banana and coffee tree. In addition, tall tress densely covering riverbanks are common. The main rivers in the area are river Chanko to the NE, Miti River to the NW, river Birbirsa to the east of the study area.

The population of the area is concentrated in settlements usually came from different nations of the country most of them speak the regional language Oromigna and Amharic. Farming and trade are the major occupation of the population. Sorghum, pepper, maize, “chat” are grown in the area. Some of the population especially that lived in the towns is engaged in handicrafts and trade.

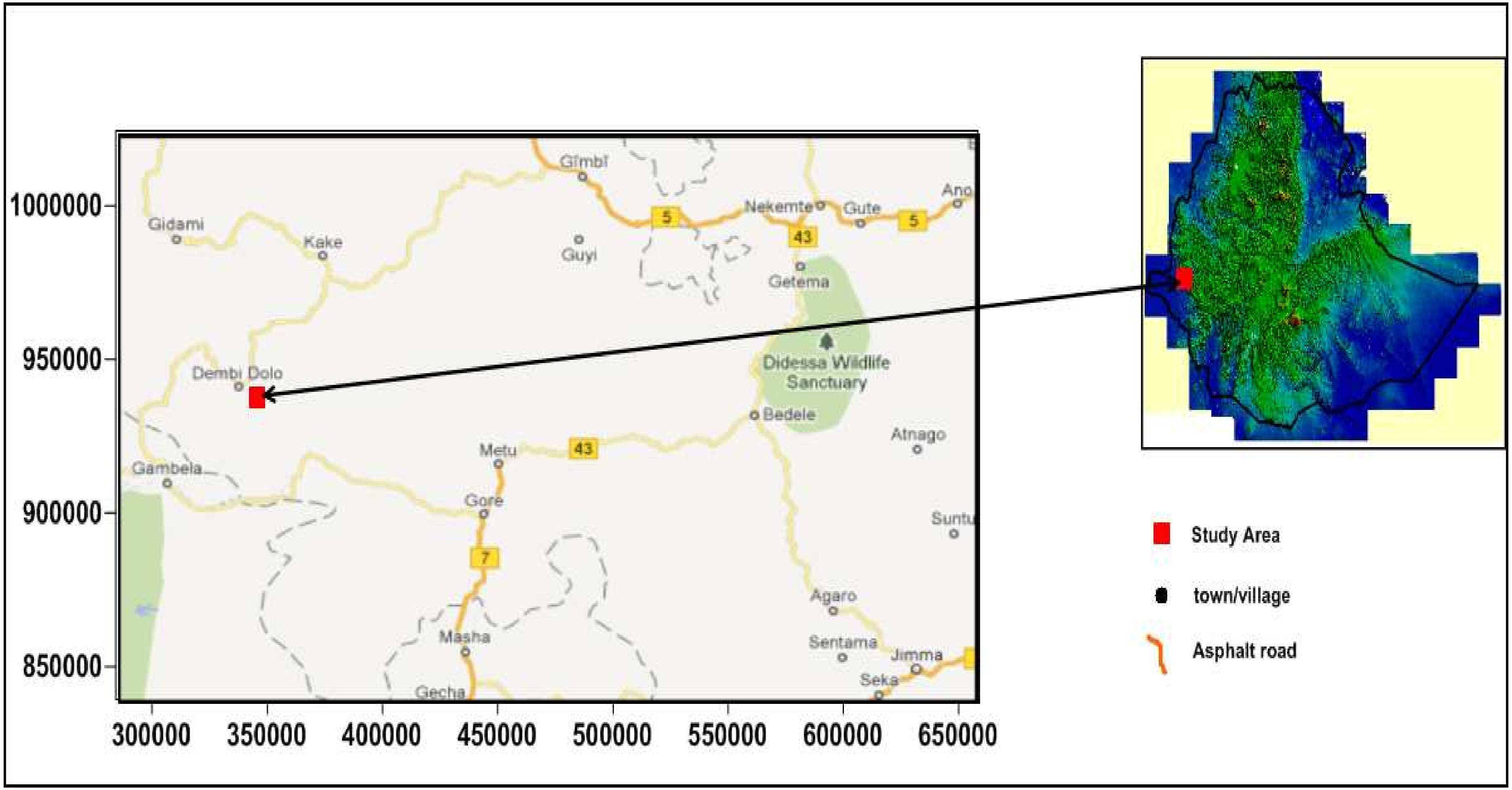

Figure 1.1 Location map of the study area in the project Area

1.3 Previous Work in the Study Area

Area selection in mineral exploration is based on the presence or absence of specific geologic features, or alternatively, geophysical or geochemical features that reflect geological features (Westerhof, 1999).

In general, geological investigations and prospecting in the study area have been carried out to a lesser extent as compared to the other gold mining belts in the country; Nevertheless, some idea of gold potential of the study area is however given in the reports of pioneer geologists who mapped some parts of the study area.

EL-Mining second year follow up report (May, 2010), presented perhaps the most comprehensive report on the geology, geochemistry of gold mineralization of the project area. According to the report, the Bir-Bir shear belt which lies at the centre of the Project area is characterized by lithological assemblages and structures (shear zones and associated dilatation related quartz veins), which are the foci for disseminated gold mineralization as is the case in most known gold mineralization zones in the country.

Most of the higher gold concentration obtained from soil and trench channel samples analyses, in third year exploration program, are mainly related to the quartz vein, altered amphibolites and sheared metaintrusives and gneisses. This suggests that both quartz veins hosted and disseminated type gold mineralization exist in the area. There have been three anomalous zones identified by soil sampling in Gute Soyoma area Zone 1 (southern), Zone 2 (central) and Zone 3 (northern). Following these findings, the third year annual report (March 2011), recommended further detail exploration work including geophysical investigations.

1.4 Problem Definition

Regional compilation, followed by some follow up and detail studies, identifies six greenstone belts in the country. These belts are identified to be continuations of the Arabian-Nubian shield and are bounded by the high-grade metamorphosed belt, the Mozambique belt. The chief sources of gold within the greenstone belts of Ethiopia comprise low-grade metamorphosed volcano-sedimentary rocks.

The Western part of Ethiopia consists of two main Greenstone belts known as the western greenstone belt and the Akobo greenstone belt. Unlike the other gold belts in the country, the western greenstone belt and the Akobo greenstone belts are less explored and studied. However, following reports of exploitation of gold and other precious metals in large quantities, these regions have recently attracted the attention of investors and researchers. In this context, the present project site is part of the area licensed by EL Mining plc for exploration of gold and other base metals and is strategically located in the junction of the above two greenstone belts.

Since the gold potential of these belts are not fully assessed, the company is currently engaged in a systematic exploration work for economic minerals in the area.

There was no geophysical data in the area prior to this work. However, before planning this geophysical work, the company had conducted regional, follow up and semi-detail geological and geochemical investigations in the area. The geological and geochemical results, from soil and trench chip samples, have showed that highly anomalous and gold values in Gute-Soyoma detail area.

Hence, the present geophysical work is planned and executed as part of the exploration program designed to locate mineral potential zones of the area by identifying prospective zones using a systematic geological, geochemical and structural mapping coupled with geophysical methods. In this framework, this manuscript deals with the integrated geophysical work conducted at selected targets of the license area in order to augment the exploration activities.

1.5 Objectives of the Present Work

General objective: The main objective of this thesis is to study the practical application of integrated geophysical methods for prospecting gold mineralization by participating in the exploration programme currently on progress in Gute-Soyoma detail area, Dembi Dolo Zone, western Wollega by EL-Mining Company.

Specific Objectives

- ❖ Detecting disseminated and/or massive sulphide minerals associated with gold mineralization,
- ❖ To map gold mineralized potential zones in the area,
- ❖ To map the lateral distribution, depth extent and dip direction of mineralized zones,
- ❖ Identifying geological structures such as faults, fractures, shear zones, etc hosting gold mineralization,
- ❖ To recommend further studies in the area in the future

1.6 Methodology

It is not usually easy to get a direct geophysical response from gold. Nevertheless, due to association of gold with particular host rock, marker beds, or structures, other indirect petrophysical indications may occur. Among the common parameters, unusual magnetization, electrical polarization, or conductivity/ resistivity can be mentioned. Mapping structures such as faults and shear zones, with which gold may be associated, is also valuable. In the present framework, the geophysical survey was, also, directed at studying and resolving these structures. Accordingly, in this study, it is planned to use integration of two geophysical methods: Magnetic and Induced polarization/resistivity (IP/Resistivity) methods.

- ➢ The magnetic method is intended to discriminate between the different lithological units. Geological structures and alteration zones are also expected to be delineated by this method. Moreover, the magnetic method can be used to locate such ores as magnetite, ilmenite, and pyrrhotite-bearing sulphide deposits.

- ➢ Disseminated or massive sulphide, thin resistive but chargeable zones such as mineralized quartz veins and other conductive minerals, can be detected and mapped using the IP/Resistivity method.

CHAPTER TWO

GEOLOGICAL BACKGROUND

2.1 Regional Geological Setting

The regional geological setting indicates that the project area is located within the western basement rock of Ethiopia. The Western Ethiopian Shied (WES) is the largest of the Precambrian cover of the country, which is similar to Arabian Nubian shield (ANS) and the Mozambique belt with in Pan- African East African orogen.

The WES characterized by a mosaic high grade Gneiss rocks separated by the north-trending low grade Volcano-Sedimentary and associated Syn-to-post-tectonic intrusions. Hence, it is believed that the low-grade metamorphic rocks and the high-grade metamorphic rocks are separated by shear zones, the western greenstone crystalline basement rocks overlain by tertiary volcanic rocks (Kazmin, et al., 1979).

The Precambrian rocks of western Ethiopia comprise wide varieties of meta-volcanic, meta-sedimentary and meta-intrusive rocks. These rocks are metamorphosed to varying degree from green schist to amphibolite facies due to multi-phase of deformations (GSE, 2000).

The project area is characterized by, three, lithotectonic Units: Baro, Geba and the Bir-Bir Domains.

The Baro and Geba Domains are composed of medium to coarse-grained quartzofeldspathic, biotite-hornblende, biotite gneisses and migmatites with no evident primary sedimentary or volcanic features (Asrat et al., 2001; Ayalew and Peccerillo, 1998; Wolde, et al., 1996, Moore et al., 1987). These rocks are metamorphosed to upper amphibolite facies as can be evidenced from the mineralogical assemblages (they lack muscovite, where as sillimanite is present with potassic feldspar in aluminous rocks and clinopyroxene coexists with hornblende in mafic rocks).

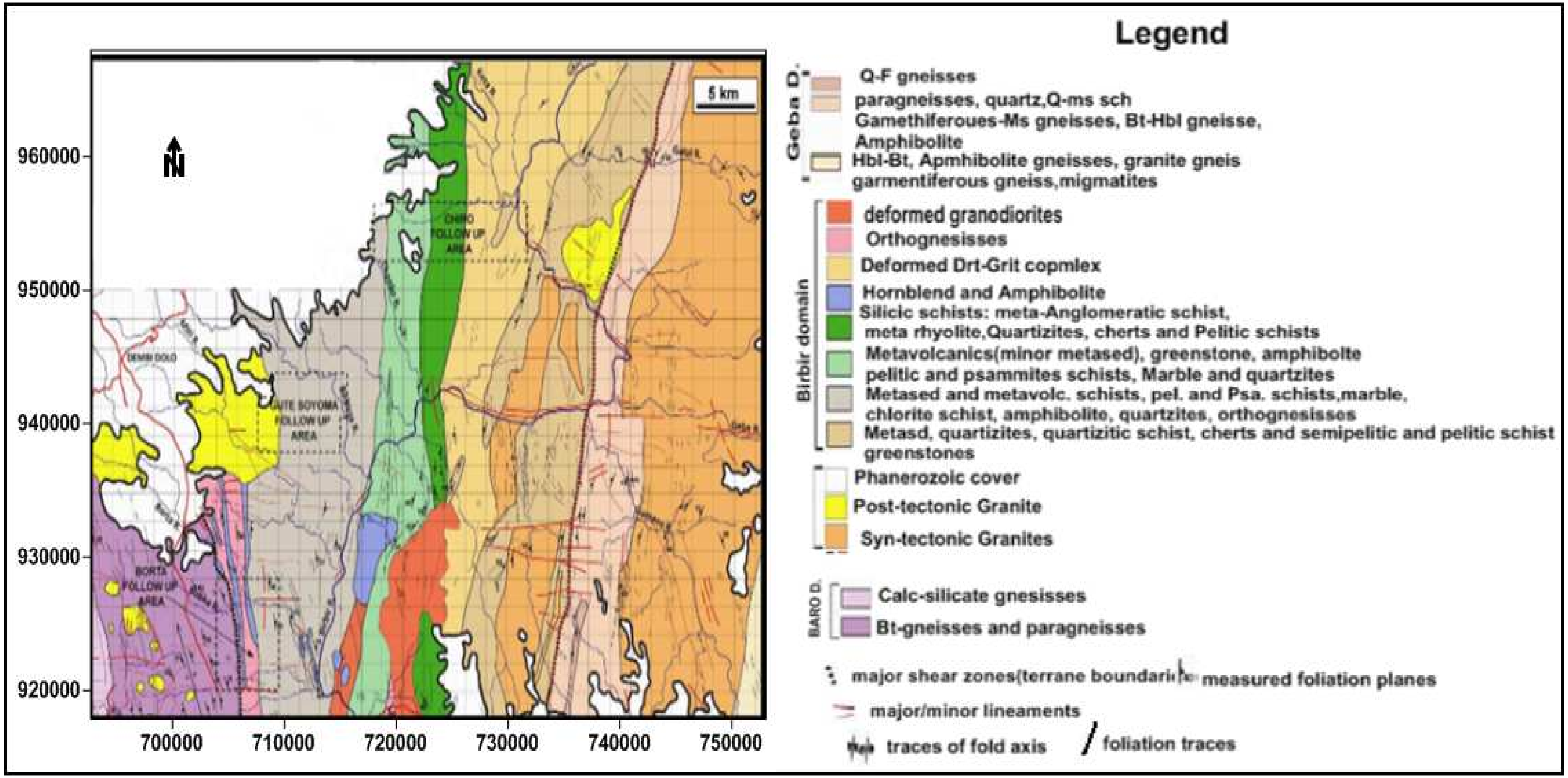

Figure 2.1 Geological map of the project area showing major structures and the location of the detail study area (EL-Mining annual report, May 2010).

- **The Bir-Bir domain** is bounded by the Baro Domain to the west and the Geba domain to, the east, and consists of an assemblage of mafic to felsic intrusive and extrusive rocks. It is the region where the present project focuses.

The Bir-Bir domain consists of basalt-andesite-dacite-rhyolite lava flows and pyroclastic flows intercalated with metagreywacke and pelite layers, which intruded by calc-alkaline plutons (granites, granodiorites, tonalities, diorites, quartz diorites, and gabbros). The Bir-Bir domain rocks are generally fine-grained schists metamorphosed to the lower amphibolite facies and locally exhibit primary sedimentary and volcanic features. They have abundant muscovite in felsic rocks, chlorite is locally stable and plagioclase is sodic even in mafic rocks, indicating a lower amphibolite facies metamorphism. It is a major transcurrent shear belt in which all rock units have been mylonitized to varying degrees and this Domain has cover most of the project area.

The central and eastern parts of the Bir-Bir Domain (most of Blocks 2 and 3 of the project area, figure 2.1) is underlain by calc-alkaline meta-volcanics intercalated with volcanogenic sediments and intruded by calc-alkaline plutons of ca 800 Ma age (Ayalew et al., 1990). These calc-alkaline meta-volcanics might indicate the site of the Proterozoic volcanic arc front (Wolde et al., 1996). This is not related to the present research.

The Western part of the Bir-Bir domain (part of Block 2 and most of Block 1 of the Project area) on the other hand, underlined by largely meta-sedimentary assemblages. These are similar to the other meta-sedimentary assemblages of the Arabian Nubian Shield to the North (e.g., Asrat et al, 2001, 2004; Vail 1983) and interpreted to be part of a sedimentary prism laid down on a rifted continental margin (Vail, 1983; Wolde, et al., 1996). This directly related to the research study area.

Three generations of plutonic rocks are recognized in the Project area. The Bir-Bir domain intruded by pre-kinematic, mafic to intermediate, pre-dominantly calc-alkaline plutons of arc affinity that range in composition from meta-gabbro to meta-tonalite and granoditoite, and deformed to varying degrees (e.g. the mylonitized hornblende and amphibolite in the western part of Block 1, and the strongly deformed granodiorite in the eastern part of Block 2). Younger, peraluminous leucogranites are common in the Baro Domain (west of Block 1), while the third group are discordant, late to post-tectonic granites of mildly alkali character that cut all the three domains (e.g., the nearly circular post-tectonic granite in Block 1). Rocks of the Bir-Bir Domain are bounded by tectonized zones; a major terrane boundary or a shear zone defines the western margin of the Bir-Bir Domain. The eastern boundary also marked by mylonite and truncation of foliation patterns. Deformation within the Bir-Bir Domain has produced penetrative foliation sub-parallel to that of the gneissic Baro and Geba domains, suggesting a coeval regional deformation affecting both the rocks of the Bir-Bir and the gneissic domains. The domains appear to have been tectonically juxtaposed, and sub-horizontal stretching lineations indicate major transcurrent movement along the boundaries (e.g., Ayalew et al., 1990; Tefera and Berhe, 1979).

The distribution of the major lithologic units in the area and the structural trends further suggest that the Bir-Bir shear belt is developed above a West-dipping subduction zone (e.g., Ayalew and Moore, 1989).

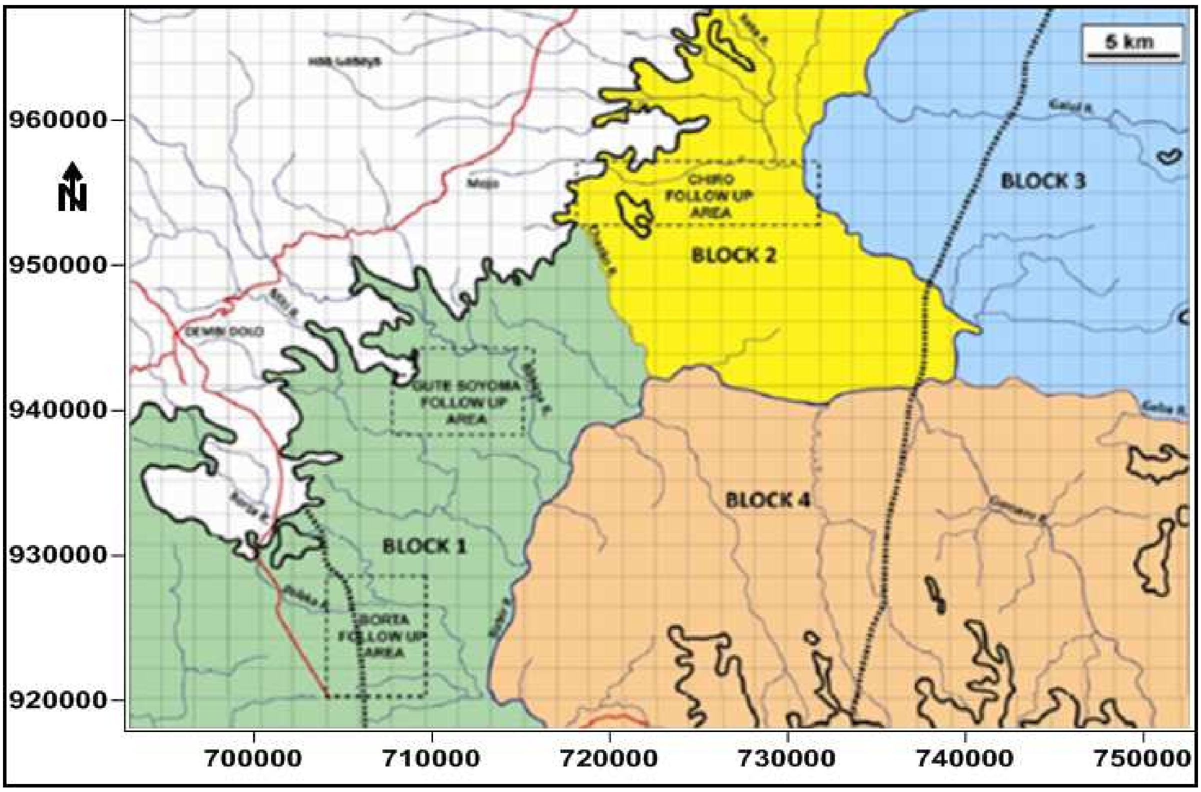

Figure 2.2 The project area`s four blocks and the location of the follow up areas (EL-Mining annual report, May 2010).

2.2 Geological Setting of the Study Area

In order to understand the actual mineralogical potential of an area like gold and base metals it is important to examine the geology of the area. Such an analysis can determine whether sufficient mineral deposits were present to justify mining work at the location.

A complete, detail and specific description of the study area, where the research specifically lies, is given by successive years end report of EL-Mining PLC. Based on the result of the EL-Mining report of May/2010 the Gute Soyoma follow up areas were delineated, a 1:25,000-scale geological map was conducted, and areas were delineated for detailed survey.

According to the report, the observed and identified geological make up of the area classified as Gneissic rocks and Metasedimentary-Metavolcanic Assemblages.

2.2.1 Gneissic Rocks

Within the Bir-Bir shear belt, the orthogneisses (granitic gneisses) are intercalated with lower amphibolite facies metasedimentary-metavolcanic assemblages and are prominently exposed in the Gute Soyoma follow up area. They are generally composed of medium to coarse-grained quartz, feldspar (dominantly microcline) and biotite. A few epidotes and sericites are also present indicating lower grade retrograde metamorphism leading to slight alteration. In many places, the granitic texture is preserved indicating an igneous origin to these rocks.

2.2.2 Metasedimentary-Metavolcanic Assemblages

These rocks form the bulk of the Bir-Bir shear belt along with deformed granodioritic and dioritic complexes and amphibolites. These assemblages are exposed in the study area.

The major rock units are Meta-sediments (pelites, quartzites, psammites [meta-siltstone, meta-sandstone and meta-conglomerate], and a few lenses of chert and marble), Bt-quartzo-feldspathic schist, meta-volcanics (meta-rhyolite, meta-andesite, meta-basalt and meta-breccia), and amphibolites and chlorite schists.

The meta-sediments are exposed in the Gute Soyoma follow up area representing the western margin of the Bir-Bir shear belt.

The metasediments (mostly thin lenses of quartzite, chert and a few marbles) are also intercalated with the metavolcanics and the amphibolites in the central and eastern margin of the Bir-Bir shear belt. These meta-sediments are generally north dipping at shallow to intermediate angles in the Gute Soyoma follow up study area, these meta-sediments are generally vertical to west dipping at high angles, suggesting a possible synclinal folding of these units with a fold axis generally trending NNE-SSW. The meta-sediments generally vary from coarser meta-conglomerates to quartzites and fine-grained slates and pelites, which show primary sedimentary layering.

Some thin layers of meta-volcanics (mostly meta-rhyolites) are exposed in the Gute Soyoma follow up area intercalated with dominantly amphibolites and chlorite schist. The meta-rhyolites depict primary volcanic features of flow banding overprinted by later foliations. These rocks are generally fine-grained rocks with few phenocrysts of plagioclase in the mafic, and microclines in the felsic varieties.

Except in few places: where some sericitization is observed, prominent alteration is absent in most of the metavolcanic rocks. The amphibolites and chlorite schists occupy major part of the Gute Soyoma follow up area intercalated with the orthogneisses at map scale. They are also associated with quartzites and meta-rhyolites. The chlorite schists and amphibolites are generally weak rocks occupying a low-lying terrain adjoining the cliff-forming orthogneisses. They form generally NNE-SSW foliated and alternatively east and west dipping assemblages suggesting a large-scale anticlinal structure. They are generally composed of hornblende and chlorites as dominant minerals with tremolites and actinolites, and some plagioclases and K-feldspars, while traces of quartz and sericites are found. Plagioclase is generally sericitized in most cases. In some areas, e.g., the site of trench 1, which is far 1.8km to the east from the study area mafic rocks (strongly altered mafic intrusive) occur as lenses within the chlorite schists and intercalated metavolcanics.

2.3 Structural Setting of the Study Area

In general, the Bir-Bir shear belt is subjected to at least four phases of deformation. The first phase of deformation (D_1) formed the S_1 foliation, which is prominent in the area and was later folded by the second phase of deformation (D2) forming S2 surfaces. However, the S2 surfaces are not readily observed except as map scale anti-formal fold axis traces. The whole sequence was later affected by D3 shearing in a general N-S to NNW-SSE direction. Such prominent shear zone marks the boundary of the Birbir shear belt with the Baro Domain gneisses in the western part of Block 1. Finally a D4 dextral brittle deformation along a generally WNW-ESE direction occurred displacing the previous deformation surfaces and in places truncating the S1 foliations.

In general, that the bulk of the foliation trends are NNE-SSW, followed by N-S trends and dominantly dipping vertically to sub-vertically towards east, although west dipping foliation planes are not uncommon.

The D4 deformation event is represented by prominent lineaments at map scale and by fractures and minor dextral faults at outcrop scale. The dominant (greater than 90% of the data) trend is WNW-ESE with vertical dipping while a few are oriented in the ENE-WSW direction. A statistically insignificant number shows other directions. In few places the dominant WNW-ESE trend are observed cutting and displacing the ENEWSW trend in a dextral sense suggesting that this deformation event was not a simple one directional brittle deformation but rather a complex sequence of events.

The two major structural trends in the area, i.e., the foliation (the folding and the shear zones are generally sub-parallel to the foliation trend) and the fracture trends are generally perpendicular to each other. From the geological investigation, it shows: all potential mineralized zones and ore bodies, associated to shear zone hosted and/or parallel to sub-parallel vein-hosted mineralized zones, are likely to be cut and displaced by the prominent fractures.

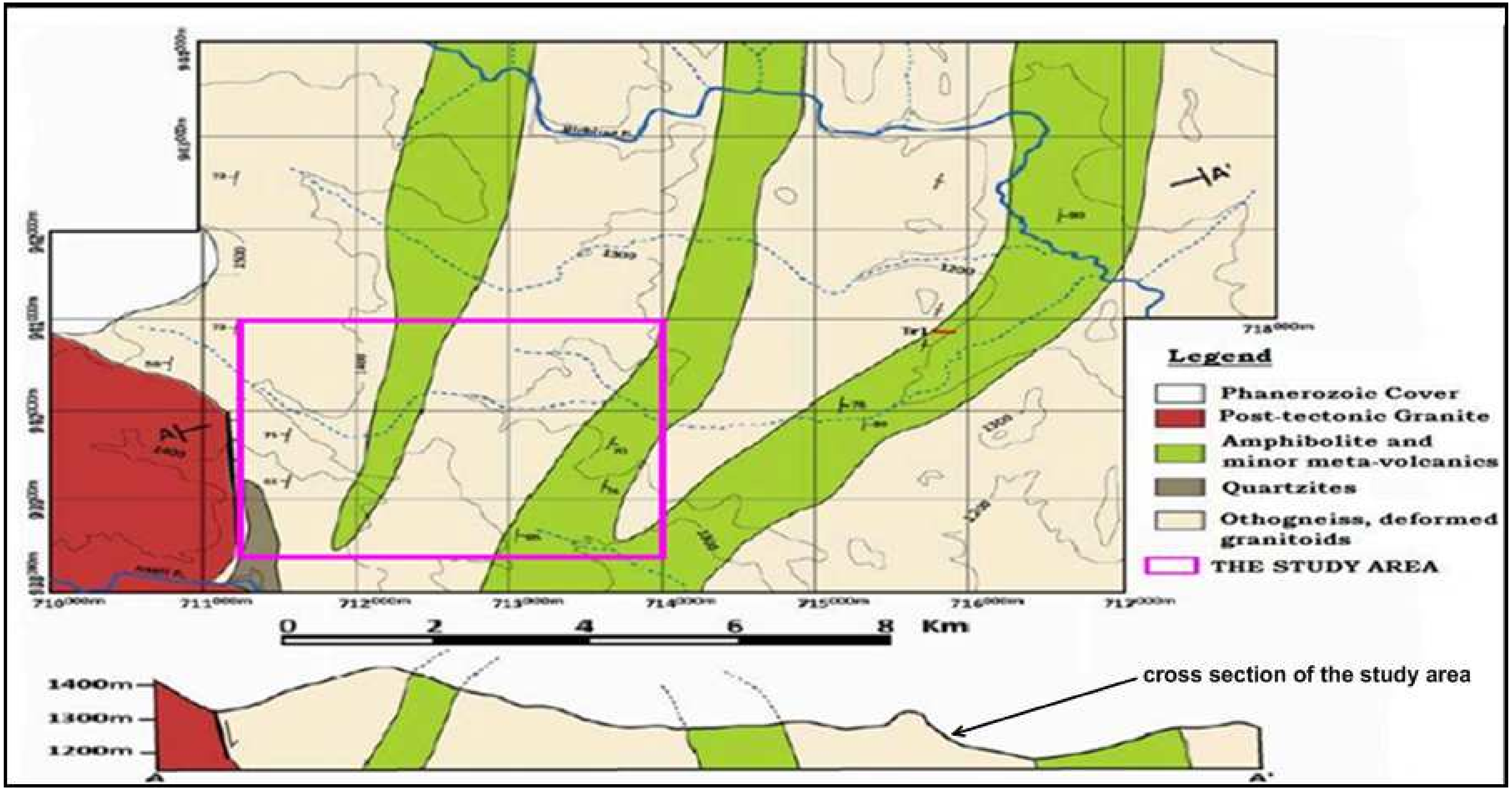

Figure 2.3 Geological map and cross section of the study area (EL-Mining annual report, May 2010).

2.4 Metamorphism and Alteration

The area is generally characterized by lower amphibolite to upper greenschist facies metamorphism of the meta-volcano-sedimentary assemblages. Lower grade (greenschist to slight alteration) metamorphism has subsequently affected some of the units. A few regional petrography studies show that the following mineral assemblage in volcano-sedimentary rocks: muscovite + biotite + quartz + sodic plagioclase in the metasediments and hornblende + biotite + quartz + sodic plagioclase + epidote in the metavolcanics. Mineral assemblages, especially the abundance of Muscovites and sodic plagioclases even in the mafic rocks (volcano-sedimentary rocks) is typical of lower amphibolite facies metamorphism. Some meta-volcano-sedimentary assemblages also contain chlorites and sericites, which might be, related either, to original greenschist facies metamorphism at the subduction fronts or, to later retrograde low-grade metamorphism. Both are possible as some of the rocks contain chlorites and epidotes as the dominant metamorphic minerals while in other cases sericites and epidotes occur around altered feldspars, and chlorites surrounding altered hornblende. This is in agreement with regional studies (e.g., Asrat et al., 2001; Ayalew et al., 1990).

No large-scale alteration has been observed in the area at outcrop scale, although chloritization, epidotization, sericitization and silicification are commonly observed at microscopic scale.

2.5 Prospecting For Gold Deposits

The earth's gold deposits were formed in all geologic epochs, from the Archean through the Cenozoic, at different stages of development with in mobile belts, platforms, and stable structures. Magmatic melts and transmagmatic solutions of various compositions have served as a source of the gold mineralization (Tatsch, et al., 1975).

Gold was among the first metals to be mined because it commonly occurs in the easily extractable native form, (Misra, 2000). Due to its relative chemical inertness, gold is usually occurring as the native metal or alloy and occasionally as large accumulations of native gold (also known as nuggets) and as in minute grains.

Commonly, gold associations are in quartz often as veins and with sulphide minerals. The most common sulphide associations are pyrite, chalcopyrite, galena, sphalerite, arsenopyrite, stibnite and pyrrhotite.

Gold deposits are formed through a wide variety of geological processes. Generally, deposits are classified as primary and placer. Primary and placer gold deposit and occurrences have been reported from the pan-Africa volcano-sedimentary sequence in southern Ethiopia (Adola, gold field), western Ethiopia (Wolega region), southwestern Ethiopia (Akobo region), and northern Ethiopia (Tigray region). (Solomon Tadesse, 2009).

Placer gold deposits form because of the breakdown and weathering of existing gold concentration of that material at a variable distance from the source to its site of deposition and concentration by a surface erosional force such as river, glaciers, oceans and (rarely) wind. Alluvial, or residual, placers are a type of placer deposit in which gold has undergone little transport and actually formed on, or near, the original source through the weathering or erosion of host rock (Solomon Tadesse, 2009).

Gold and its many alloys are most often used in jewelry, coinage and as a standard for monetary exchange in various countries. When selling it in the form of jewelry, gold is measured in karats (k), with pure gold being 24k, 21k, 18k and 14k. A lower “k” indicates a higher % of copper or silver mixed in to the alloy, silver being the more commonly used metal between the two (Solomon Tadesse, 2009).

2.6 Indications of Gold Mineralization in the study area

The geological-structural setup of the area is fertile for gold mineralization as it is has similar setting to known mineralized provinces in the country (e.g., southern Ethiopia). Due to the following indications:

- **Placer gold mining activity and presence of placer deposits:** Placer gold mining activity in various parts of the Birbir shear belt following the tributaries of the Birbir River has been known for long time. Residents are engaged in full- or part-time placer mining activity in the Birbirsa and Meti rivers and reports from miners and first hand observations indicate that a considerable amount of gold is mined through traditional panning. A thin, 30 cm thick conglomeratic placer deposit is also observed at the eastern bank of the Birbirsa River. Any primary gold deposit should be located within the metavolcano-sedimentary assemblages drained by these rivers.

- **Quartz veins and veinlets**: ranging in thickness (width) from a few mm to about 3m and extending along their length from a few cm to tens of meters are abundant in the Birbir shear belt in general and the study area in particular. They generally trending along the foliation directions of the enclosing rocks and sulphidized with observable pyrites and chalcopyrites and some have oxidized rust vugs. A few glassy white discordant lensoid veins are also present in few localities.
- **Geochemical anomaly (Soil Chip and Channel samples)**

The soil, chip and channel samples were analyzed for gold at the Ethiopian Geological Survey Central Laboratory by using AAS (Atomic Absorption Spectrophotmetry). The trench is dug across an altered amphibolite with many sub-parallel sulphidized and oxidized quartz veins, and a few lenses of meta-rhyolites, and located close to the contact with orthogneisses. The overburden is not thick and is generally less than a meter. The floor of the trench was sampled at every 1 m interval and 50 samples weighing in excess of 0.5 kg each were collected for chemical analysis. No panning was conducted. 7 chip samples and 50 channel samples were collected from the quartz veins exposed at the wall, floor of the trench 25-channel samples were analyzed and the results are returned. All the 25 channel samples returned gold values ranging from 12 to 68 ppb and mean values 25 ppb, 12 samples with Au values show below mean and 13 samples above mean value. Among the 4 intervals, especially the intervals 2-9 m, 21-29 m and 46-49 m show continuously high gold values for 8, 9 and 4 m, respectively; and anomalous values for 4, 7 and 3 meters, respectively. In conclusions of the result, (1) the rock assemblage represented by this trench is mineralized with gold; (2) the source of the gold is the altered amphibolites and sulphidized quartz veins and veinlets; (3) the gold mineralization is a disseminated and quartz vein hosted type.

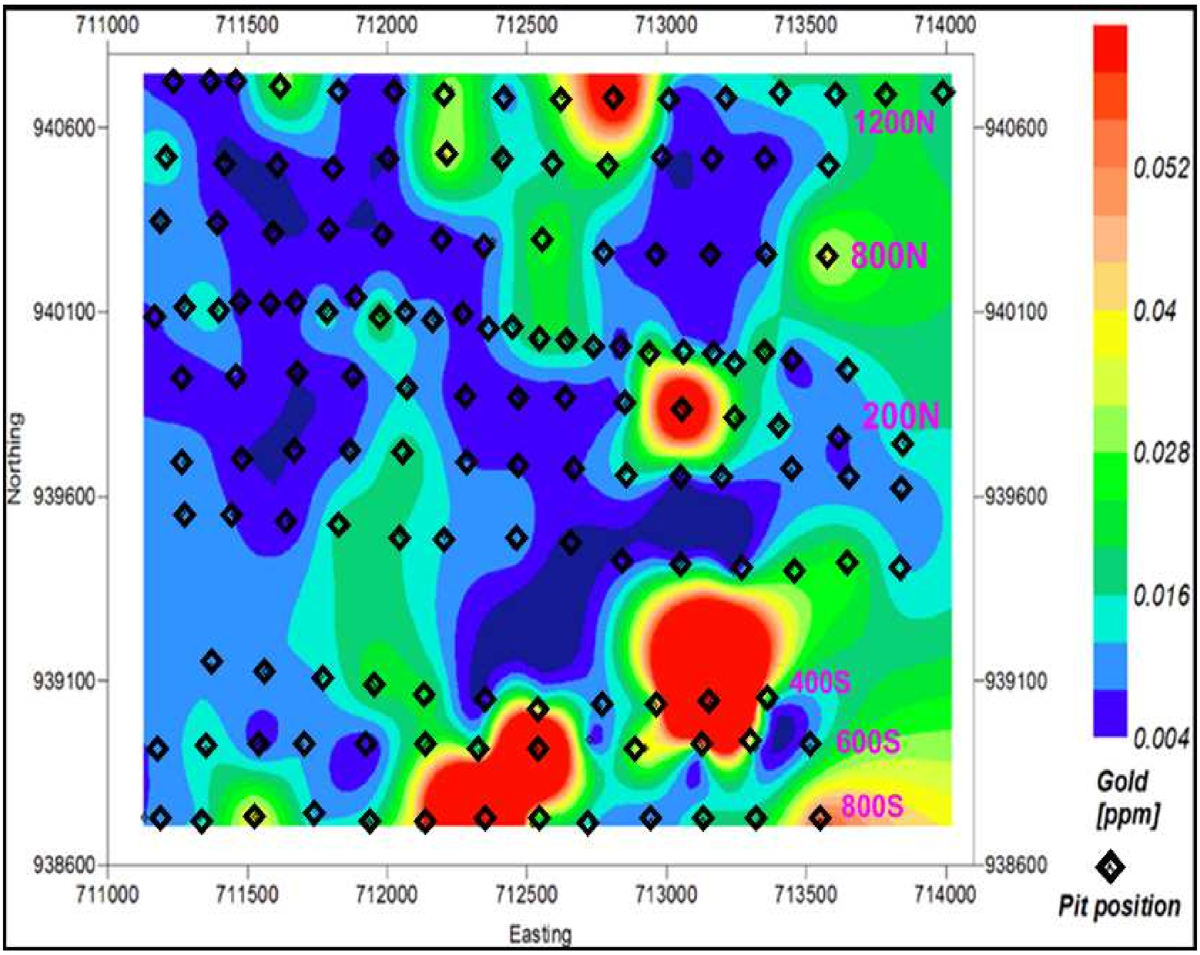

Figure 2.4 Geochemical map of the study area and IP/Resistivity lines (EL-Mining annual report, March 2011)

The soil geochemical results of the total area were presented as gold anomaly map and at least four strong gold concentrations were identified. These high AU anomalies are located in the northern tip between 712500 to 71300 and the second at the central east, the third and the fourth are at the southern side between 71200 and 713500. However, at the flank of SSE part of the area moderate signature up to 0.045ppm is detected. Those all high gold anomalies have showed (>0.052ppm) gold values and situated at the contact of the orthogneisses and altered amphibolites. The remaining part of the area showed low gold anomalies. As a result, most of the geophysical surveys (numbered lines) were conducted over high gold value regions (figure 2.4) (EL-Mining annual report, March 2011).

CHAPTER THREE

GEOPHYSICAL DATA ACQUISITION AND PROCESSING

3 General

In order to map the mineralized zone of the project using integrated geophysical techniques, a fieldwork for ground investigation was planned and executed by EL-Mining plc. The fieldwork was carried out from 10th to 18th February, 2011. During the fieldwork, ground magnetic and IP/Res data were collected. Magnetic data were collected along eight profiles approximately 2km long each while the IP/Res were collected on six lines based on the previous detailed geochemical and geological reconnaissance surveys (figure 4.1).

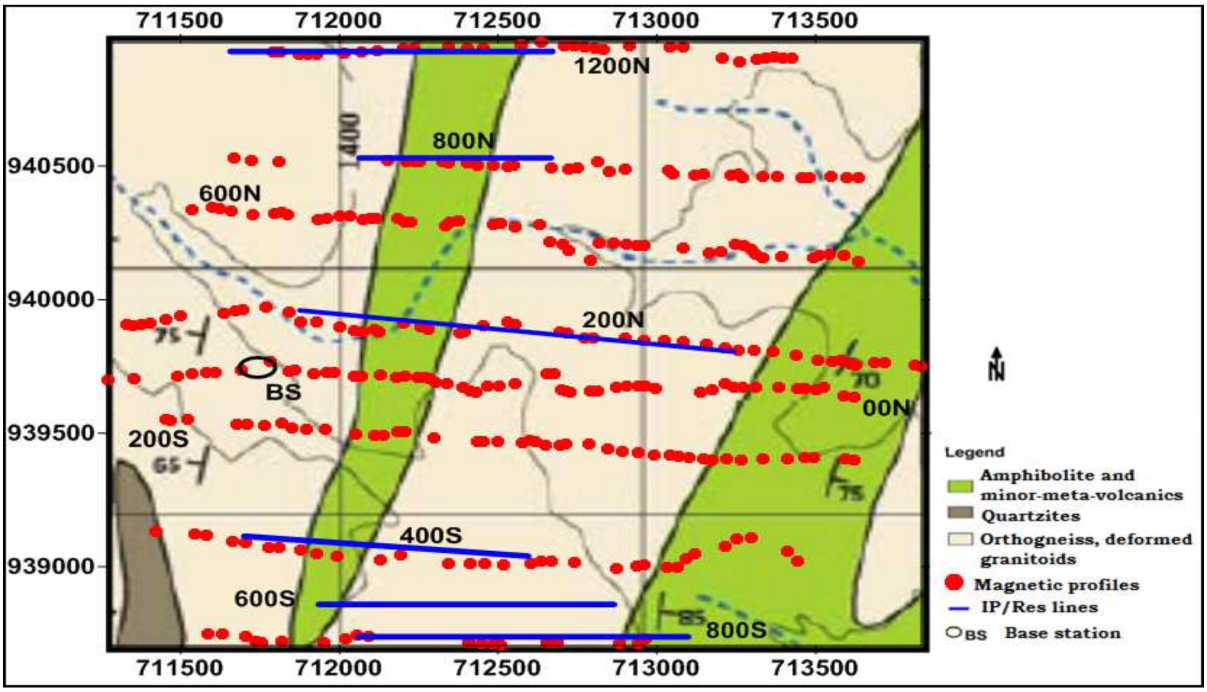

Figure 3.1 Magnetic profile and IP/Resistivity lines on geological map of the study area.

3.1 The Electrical IP/Resistivity Survey

3.1.1 Instrumentation

The resistivity equipment used in this project was IRIS Instrument SYSCAL R1 PLUS Switch-72 that is a new all-in-one multiple resistivity imaging system. It designed for medium depth investigation. It is made up of a power source that transmits up to 600V output voltage and a receiver unit.

It consists of an internal switching board for 72 electrodes and an internal 200W power source. It is compact, easy to use and field proof. The SYSCAL R1 PLUS Switch-72 measures both resistivity and chargeability (IP) simultaneously.

3.1.2 IP/Resistivity Field Procedures

The 2D resistivity profiles data survey were conducted along six survey lines oriented approximately east- west with in the area. The array used in the area was a hybrid array, which is called Wenner- Shelumberger. The length of a single profile achieved during the survey was 360m using 4 cables (18 electrodes each) with 10m separation. In order to increase the lateral extent of the profile roll along was performed.

Along all profiles, a total of six main sequences and forty-one roll along were acquired in the study area. The instrument simultaneously measures apparent resistivity and chargeability then stores in its internal memory. During the measurement, one main sequence collects 223 data and a single roll along adds additional 100 data.

The IP/Res measurements were not started and ended at a fixed position. It was depending on the result of the geochemistry and geological investigation on previous reconnaissance survey.

3.1.3 IP/Resistivity Data Processing and Presentation

Processing is required in order to transform the geophysical data so that it can be interpreted geologically. After the data acquisition, the measured apparent resistivity and chargeability data were uploaded from the memory of the IRIS instrument, (SYSCAL) using downloading software called Prosys II for further processing and analysis. In this software, data from roll along sequence were added to the main sequence data. Topography data were also inserted and the apparent resistivity values recalculated, before exporting the data for further processing and inversion. On Prosys II, selection of the type of array used and modification of electrode spacing were done. At a starting stage for processing, automatic filtering technique was used for the elimination of outliers (noise).

For further processing, the data were export and save in RES2DINV format. The apparent resistivity and apparent chargeability pseudosection and inverse model section maps, along all profiles, were prepared by using RES2DINV software.

In principle, the measured data during electrical survey is the bulk resistivity of the subsurface, which is also known as apparent resistivity. Since most investigations are not aimed at knowing the bulk subsurface parameter but the subsurface layers resistivity distribution, there is need for an efficient and accurate inversion method. Resistivity inversion can simply be defined as the process of re-constructing subsurface resistivity distribution from the measured apparent resistivity or voltage data advanced geosciences inc. (AGI, 2008). The inversion of resistivity data has dominated the convectional curve matching process for determining the subsurface true resistivity. Application of inversion program to the measured apparent resistivity enable clear interpretation of the Earth`s resistivity structure (Boonchaisuk et al, 2008).

In geophysical inversion, we seek a model that gives a response which is similar to the actual measured values. The model is an idealized mathematical representation of a section of the earth, which has a set of physical parameters that represent the observed data. The model response is the synthetic data that can be calculated from the mathematical relationships defining the model for a given set of model parameters. All inversion methods essentially try to determine a model for the subsurface whose response agrees with the measured data subject to certain restrictions. In the cell-based method used by the RES2DINV program, the model parameters are the resistivity values of the model cells, while the data is the measured apparent resistivity values. The mathematical link between the model parameters and the model response for the 2-D resistivity models is provided by the finite-difference (Dey and Morrison 1979a, 1979b) or finite-element methods (Silvester and Ferrari 1990).

The exported apparent resistivity data for the six profiles were inverted in the RES2DINV software; the software automatically calculates the subsurface true resistivity using various inversion settings. In this research, the inversion of the resistivity and IP data is conducted by Least-square inversion by involving finite-element and finite-difference methods. The technique is based on the assumption of linear distribution of data error; it has been found to be very effective inversion method for noisy data (AGI, 2008).

In order to achieve a better and accurate subsurface imaging, with relatively low Root Mean Square Error (RMSE) for different number of iterations, the inversion procedures were generated. The results of the resistivity and IP inversion and their interpretation are displayed in inverted model section and interpreted stacked plan map forms. During the process, logarithmic and customized linear contour intervals are used for resistivity and IP respectively.

3.2 The Magnetic Survey

The success of magnetic survey, in the context of mineral exploration, depends mainly on the accuracy achieved during the field measurement. Basic requirements for an accurate data set are quality of the magnetometers, a well-designed survey, high precision careful measurements, and state of the art data processing (Kirsch, R., 2006).

3.2.1 Instrumentation

The instrument used for magnetic survey is the Geometrics 856 Proton Precision Magnetometer. It measures the absolute value of total magnetic field to a resolution of $0.1nT$ with accuracy of $0.5nT$. It has memory storage, and gradiometer option for geologic mapping and archaeology. It is used in various field applications such as fault and geological mapping, mining and location of magnetic minerals.

It is made up of six-digit display of the magnetic field and three-digit display of station, line number and signal strength. Geometrics 856 Proton Precision Magnetometer uses 9D cell industrial grade batteries and it is connected to magnetics coils mounted on the pole for measurement. The G-856 has two parts of operation--auto (automatic) mode and survey mode (regular field operation where the operator pushes buttons to take a reading).

3.2.2 Magnetic Data Acquisition

The magnetic data were collected perpendicular to the strike along eight selected lines in the study area oriented approximately East- West in direction. The two profiles (00N, 200N) collected covered a lateral distance of 2.5km and separated by a distance of 200m while profiles (200S, 600N) covered a lateral distance of 2.2km and also profiles (400S, 800N) covered a distance of 2km, profile (800S, 1200N) covered 1.5km and 1.8km lateral distance respectively. Note, all profiles were run in west-east direction.

Before any measurement taken a fixed base station for all profiles was established at 00N of coordinate (711671E, 939742N) and the instrument was checked for batteries, then test two or three measurements to check if there was a magnetic storm in that day. However, throughout the measurement there was not storm at all. In this survey, one magnetometer was used for the field and for base station reading. The reading was taken on foot and reoccupied every one or two hour interval for the purpose of diurnal correction. Six hundred twenty (620) data were collected from the eight lines with 20m station interval.

The accurate positions of the magnetic data points were determined using the latest version hand-held GPS (Global Positioning System). The GPS used was Garmin **e** Trex Legend. This GPS can locate the coordinate of the area along with the elevation (less than 2m of accuracy) in the lower section of the satellite page, which is essentially needed in the magnetic reductions.

3.2.3 Magnetic Data Processing

The collected data should be processed for effective interpretation of the subsurface mineralized zones (faults and fractures) geometry. Thus, the raw Mag data collected on the field sheet were transferred on the excel sheet for diurnal and IGRF corrections.

3.2.3.1 Diurnal Variation Correction

After the data collection, the diurnal effect was calculated from a fixed base station and the magnetic data were filtered in order to correct for drift or diurnal effect in the magnetic readings. Noise due to secular change or epoch was considered negligible because consistent measurements were taken at the base station every one or two hour.

3.2.3.2 Calculation and Removal of the Geomagnetic Field

After correcting the observed total field magnetic data for the diurnal effect, the theoretical geomagnetic field (IGRF), for the duration of the survey and for that specific location was determined from the online geomagnetic data center (NOAA, (http://ngdc.noaa.gov/geomagmodels/struts/IgrfWmmLocationSwitch)]. The model is calculated based on the dates, elevation and geographical locations (latitude and longitude) of the observed magnetic data which gave the average geomagnetic field of $35115.3nT$**,** inclination of -0.767^{O} and declination of 2.23^{O} of the study area. The IGRF was then subtracted from the observed magnetic values for each station to determine the residual magnetic field due to anomalous contribution from local magnetic sources in the area.

3.2.4 Magnetic Data Presentation

After the removal of all corrections, the residual data were processed and plotted on 2D contouring, gridding and mapping software: Oasis montaj. The results are presented in contoured forms for visualization and further enhancements. For 2D visualization, the total magnetic field intensity data were gridded using minimum curvature gridding method with 50m cell size and 250 blanking distance.

For effective interpretation of the obtaining magnetic data, further enhancements were carried out using various transformations such as, analytical signal; vertical derivative and Tilt derivative are used. The transformations are made using a mathematical property of potential fields that allows 2D maps of any component of a field to be transformed into maps of the same component or into maps of another component, or into maps of the gradients.

CHAPTER FOUR

DISCUSSION OF RESULTS AND INTERPRETATION

4. Results and Interpretations of Different Anomaly Maps

The carefully and thoroughly processed geophysical data were used to produce different anomaly maps, which show contrast in the resistivity, chargeability and susceptibility of the subsurface rocks. The following section will show the results and interpretation of magnetic anomaly IP/Resistivity and maps.

4.1 Total Observed Magnetic Field Intensity Map

The total observed magnetic field anomaly map was created after the diurnal corrections and removal of the IGRF model field from the field-collected data, figure 4.1.

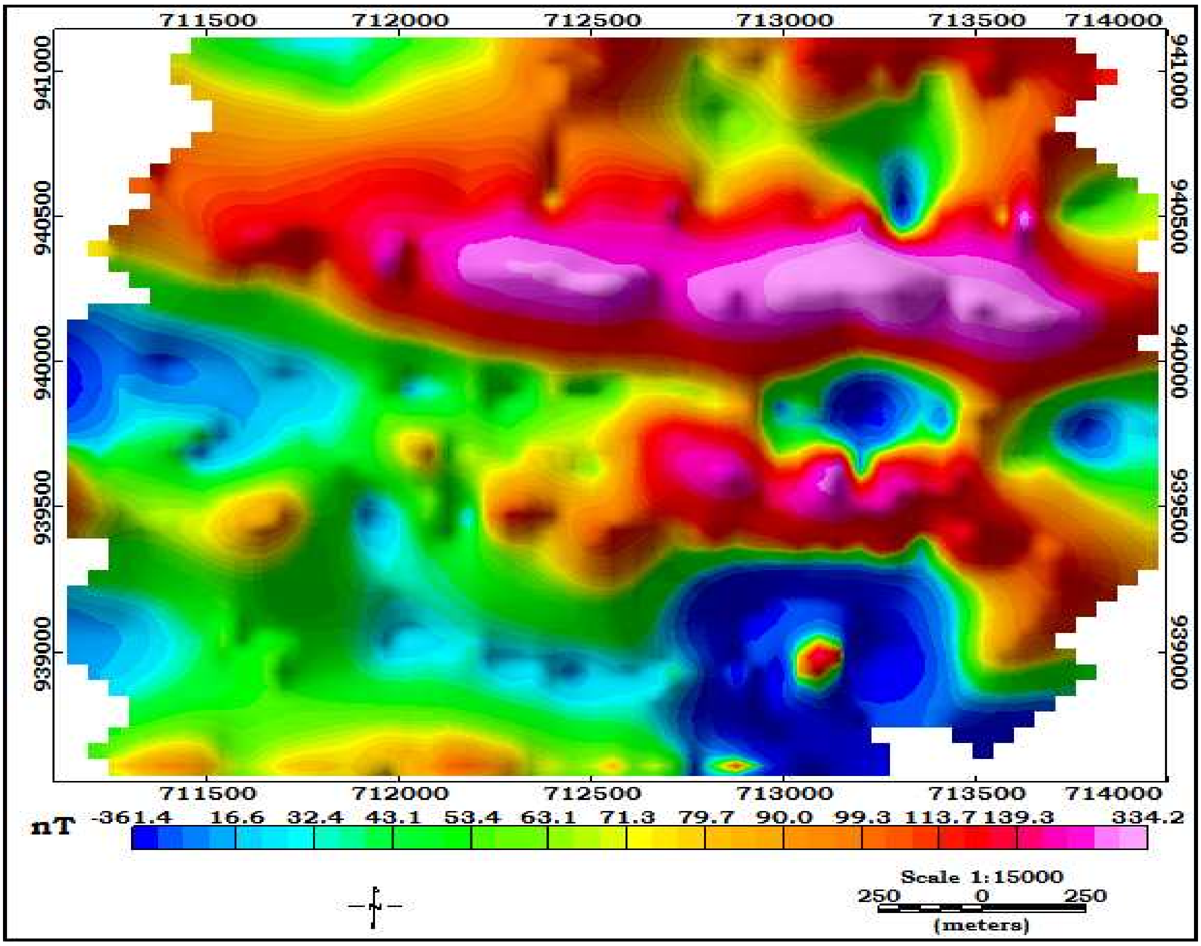

Figure 4.1 Total observed ground magnetic field intensity map

As shown in the map, the total magnetic field intensity varies from -361.4 to $334.2nT$.

An interpretation difficulty with TMFI anomalies is that they are dipolar (anomalies having positive and negative components) such that the shape and phase of the anomaly depends in part on the magnetic inclination and the presence of any remnant magnetization. This anomaly complexity makes interpretation more difficult because the body and its edges do not necessarily coincide with the most obvious mapped feature.

Hence, in order to accentuate the magnetic signature of the mineralized zones and associated structures, analytic signal has been calculated from TMFI values and interpretations were made based on these map results. In addition, first vertical derivative, TDR (Tilt Derivative) magnetic maps were prepared from analytic signal values.

4.2 Analytical signal map

The analytic signal is useful for locating the edge of magnetized bodies in areas of low magnetic latitude. Absolute analytic signal according to Roest et al. (1992) defined as the square root of the squared sum of the vertical and the horizontal derivatives of the magnetic field. The analytic signal generates a maximum directly over discrete bodies as well as their edges. The maximum width of a, or ridge, is an indicator of depth of the contact, as long as the signal arising from a single contact can be resolved. An important characteristic of the analytic signal is that it is independent of the direction of the magnetization of the source. (Macleod et al., 1993)

Analytic signal maps seems to be more useful than reduction to the pole, as they are not subjected to the instability that occurs in the transformation of magnetic fields from low magnetic latitudes, they also define source positions regardless of any remanence in the source. The strength/amplitude of an AS anomaly is also proportional to the susceptibility of the causative body i.e. the greater the proportion of magnetic minerals in the body the larger the AS anomaly. It is also useful for structural interpretation.

In the total observed magnetic map there are two dipolar anomalies presented which by application of the analytic signal this dipolar pattern has been removed completely (figure 4.2).

High amplitudes that have greater than 0.8nT/m are detected at SSE between coordinates 713000-714000, at the flank of WNW, and moderate anomaly signature at the central region of the area. The high response at the western and at the flank of WNW is possibly the effect of the post-tectonic granite and phanerozoic cover respectively where as N-S trending high anomaly on the eastern side might be the effect of amphibolite and minor metavolcanics. Very low responses, whose value less than 0.8nT/m lie on the local geology of orthogneisses. Therefore, the analytic signal magnetic clearly identifies proportion of magnetic minerals in the local geology.

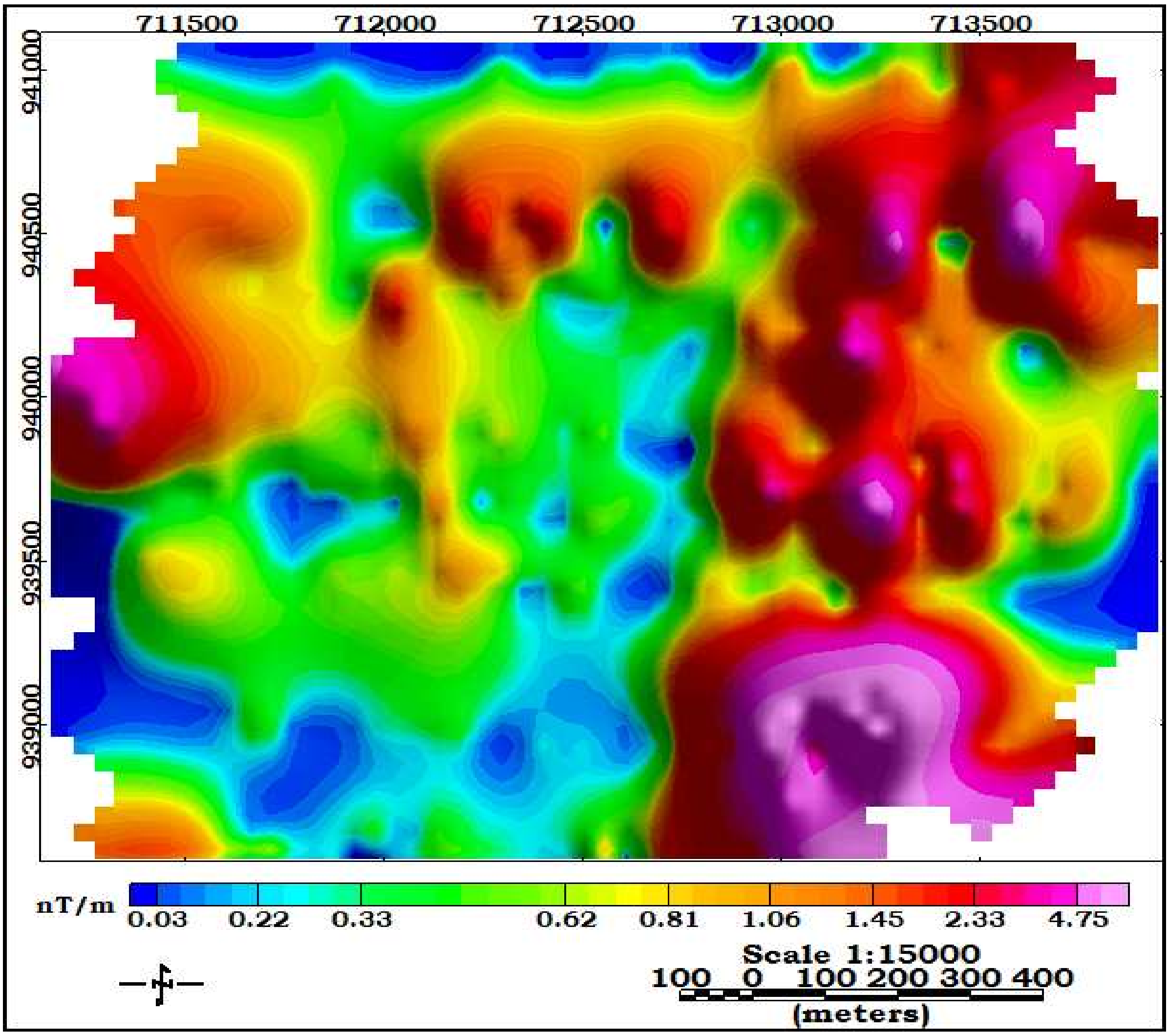

Figure 4.2 Analytic signals map

It also shows maxima over the contact (figure 4.2) at the eastern part of the study area trending NW-SE direction. Moreover, the analytic signal clearly shows a magnetic contacts or indicating a structure possibly, though which the mineralised fluids raised. As indicated in the figure, the contact is broad at the south end and becomes gradually narrow to the north, suggesting the discrete bodies are deep seated and slightly exposed at the northern than to the southern part of the area. These high signatures are also detected at the NNW and SSE flank of the area. The high amplitude of the analytic signal at the eastern region shows discontinuities from south to the north, this discontinuity might be due to shearing effect.

4.2.1 First Vertical Derivative Map of Analytic signal

The first vertical derivative of the analytic signal sharpens the image resolution and defines the positions of anomalies more clearly. These features, together with enhancement of the signal from shallow sources, make it potentially of valuable in interpreting the sources.

It is the derivative of the analytic signal in z-direction and as such outlined the very high amplitude, discontinuous features that are NNE-SSW trending at the eastern and WNW flanks. Moreover, less intensified moderate responses at the central region of the area are from amphibolites and minor meta-volcanics. However, low anomalies are from the responses of orthogneisses that might have no magnetite minerals inside them.

High magnetization is usually associated to rocks containing ferromagnetic minerals. For instance, basic igneous rocks contain these minerals and show high response. Intermediate and low magnetic responses may correlate with metasediments. At the eastern side, the high magnetic responses are displaced laterally and cut by E-W trending fractures and minor fault, figure 4.3.

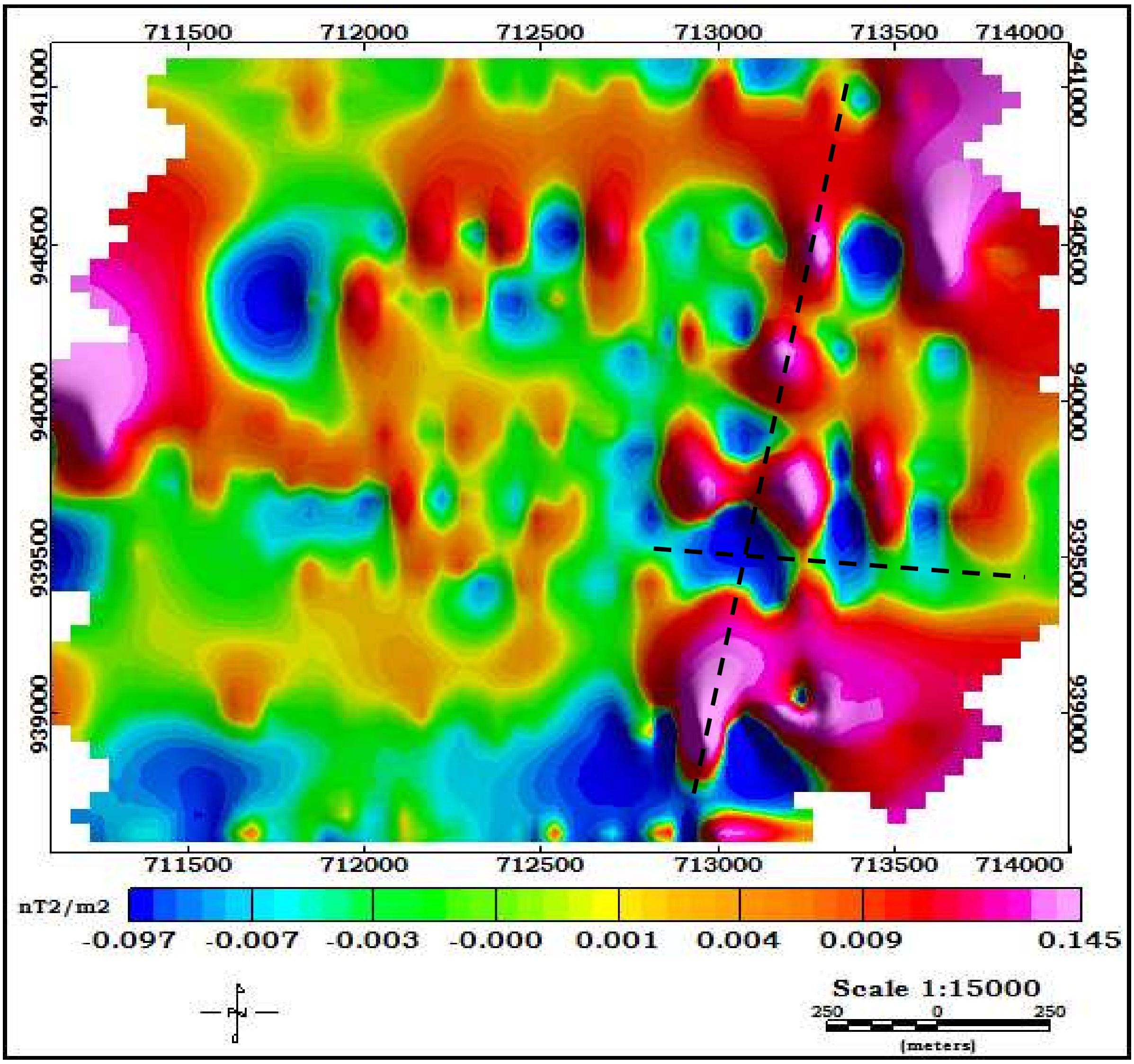

Figure 4.3 First vertical derivative of the analytic signal.

4.2.2 Tilt Derivative of the Analytic Signal Map

One of the major features of the tilt derivative is that it is very effective in tracing out anomalies along the strike. This is because the filter uses an automatic gain control, which tends to equalize the response from both weak and strong magnetic anomalies. Since the strike direction in the study area is almost N-S in direction it is likely to observe these features clearly on figure 4.4. In the picture NNW-SSE, N-S and some NNE-SSW trending anomaly features, sheared zones and E-W trending fractures and minor faults are mapped. Moreover, these magnetic responses showed that how much lateral movement affects the area geology.

Since characteristics of the magnetic response largely depends on concentration of magnetic minerals present, the geometry and depth of the deposit, its orientation relative to the magnetic north and the inclination of the earth`s field at its location.

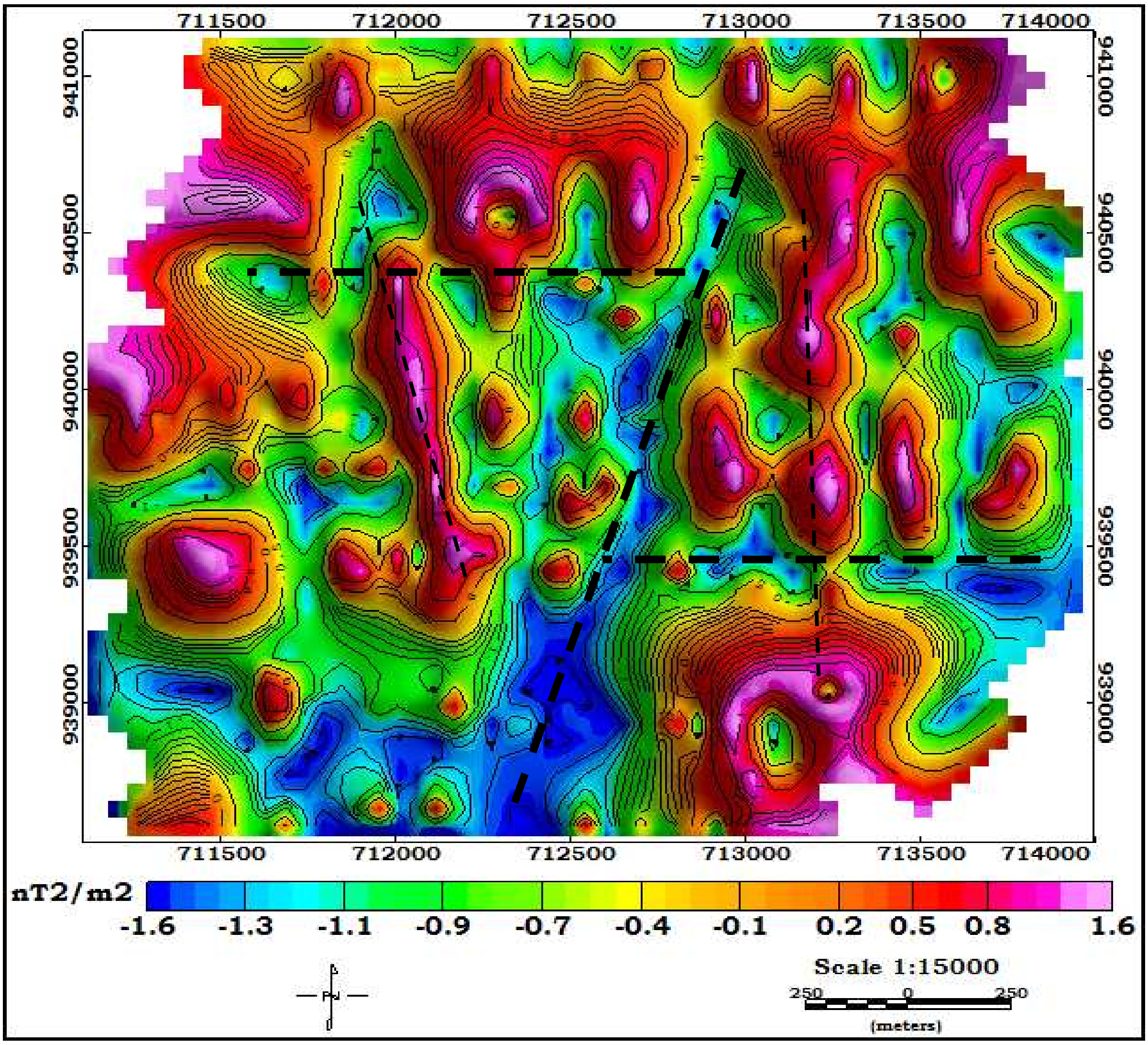

Figure 4.4 Tilt derivative of the analytic signal

Magnetic anomalies associated with gold mineralization itself may be due to metallic sulphides, either magnetite or pyrrhotite. The anomaly may be positive or negative depending on weather the process of mineralization has enriched or destroyed these minerals. The sulphide that may be associated with gold mineralization depends on the local metamorphic grade. In greenschist facies, pyrite or arsenopyrite is expected. However, at the amphibolite facies either pyrite or pyrrhotite may be dominant (Groves et al. 1990).

Thus, depending on their magnetic magnitude and the signature shown on figure 4.4, the responses are grouped into high, moderate and low.

Therefore, very high magnetic responses that values greater than $-0.4nT2/m2$ are detected at western, central and eastern on the amphibolites and minor meta-volcanics.

This high magnetic amplitude of the signal possibly result from the high content of magnetite/pyrrhotite or other magnetic minerals (base metals) basic igneous rocks in this part of the rock units since these substances have high susceptibility, the response for the magnetic measurement is positive. These anomalies are trending in N-S, NNW-SSE directions following the foliation trend of the area.

Moreover, the long wavelength anomalies observed on the figure are the response of the rocks from the depth whereas the short wave length anomalies believed to be the response from the shallower features. And also high zigzagged and lines indicates the shearing effect of the rock units.

The second kind of magnetic response is the area where moderate magnetic anomalies and their signature of their value ranges from$-1.1nT2/m2\ -0.4nT2/m2$. This signature observed mostly on the gneissic rocks and metasedimentary-metavolcanic assemblages. The magnetic amplitude observed on the amphibolite and minor-metavolcanics are moderately high, the discontinuity of the amplitude is due to shearing.

The third magnetic characteristic is the area where low magnetic amplitude detected and has values less than -1.1nT. The signatures are lies on orthogenesis. The low magnetic anomaly areas can be interpreted in terms of the responses from highly demagnetized subsurface rocks.

Although, no large-scale alteration has observed at map scale in the area, there are presences of alteration at microscopic level in the area. Among of them altered amphibolite, hornblende and feldspar are common. Therefore, thus rocks may lose their magnetite content. This anomaly indicates that the rocks in this part have low susceptibilities indicating that no magnetic minerals or lose their magnetic content.

In conclusion, most of the magnetic high responses are coincide with the gold geochemical anomaly map of the area. However, high magnetic signatures, which are not observed on the gold map, are manifested on the magnetic map. This high signature has possibly the existence of other minerals other than gold but likely base metals. Moreover, low and moderate responses are detected to the southern part of the area however; high gold anomaly is occurred on geochemical result, which is not fully associated with the magnetic response. This low and moderate magnetic, high IP/Resistivity and high geochemical results possibly indicates pyrite mineralization in that region.

4.3 IP/Resistivity result discussion and interpretations

4.3.1 IP/Resistivity Inverse Model Section 800S

This profile covers total length of 980m with 10m electrode spacing and is shown, on the inverted model, penetrating to a depth of 67.5m, figure 4.5. The ground surface shows a steep rise up to station 320m and then drops to the west.

The 2D resistivity model section is characterised by relatively moderate to high resistivity distributions with the highest value 4568 Ω.m. Most of this profile lies on the orthogenesis and a few on the amphibolite to the eastern side of the profile. On the map, there is an increase in resistivity values from near surface to the bottom of the profile and structures which are trending NNW-SSE are identified in the profile approximately at 230m, 440m, 640m and 730m. These structural signatures, revealed on the inverse model may reflect the tectonic features that affected the area i.e. the rock units in the area are highly folded and sheared due to tectonic activities happened in the area; it also proves that the area is metamorphic terrain. Moreover, the progressive increase in formation resistivity may indicate that the decrease in degree of weathering of the rock units from the surface to higher depth.

The overall picture of the 2D resistivity depth model reveals the presence of four prominently resistive zones within a vast moderately conductive subsurface. The four-resistivity zones lies between 0m and 200m, 320m and 430m, 480m and 720m, 910m and 960m. These high resistive and IP anomalies correspond to the magnetic high of the Analytic Signal and may represent magnetic minerals hosted in quartz veins.

There are also IP anomalies of different amplitude present on this line. The first prominent IP anomaly lies between stations 320m and 450m. This anomaly has a highest IP response (>25mV/V) and spatially corresponds to the second high resistive zone. The top of this feature appears at a depth of about 48 meters and possibly extends to the larger depth. The other deep-seated moderate anomaly of interest lies between 110m and 130m and tends to deepen and broaden to the west. The deepest anomaly was also detected beneath station 210m, at a depth of about 59 meters and occurs on the displaced high resistive zone.

There also appear one shallower anomaly at the stations between 530m and 580m, and two smaller anomalies in a discontinuous manner. These anomies lies on the resistivity change (moderate to low), indicating possibly the presence of sulphide material hosted in quartz veins and veinlets. In general, the high IP anomalies on this line are associated to the resistivity highs.

At the subsurface of the area, fractured and weathered boulders are manifested. The high resistivity of the rocks showed increasing its amplitude to the centre of the body and also for the IP anomaly. This high IP/resistivity may indicate a quartz vein mineralization. The second very high IP anomaly is found over the low resistivity zone (high conductivity) possibly attributed to the sulphide mineralization hosted in quartz veins. Geological and geochemical studies have shown that the sulphide mineralization is typically fined-grained and disseminated through the quartz veins, which are all hosted by the amphibole schist (El Mining third year exploration report).

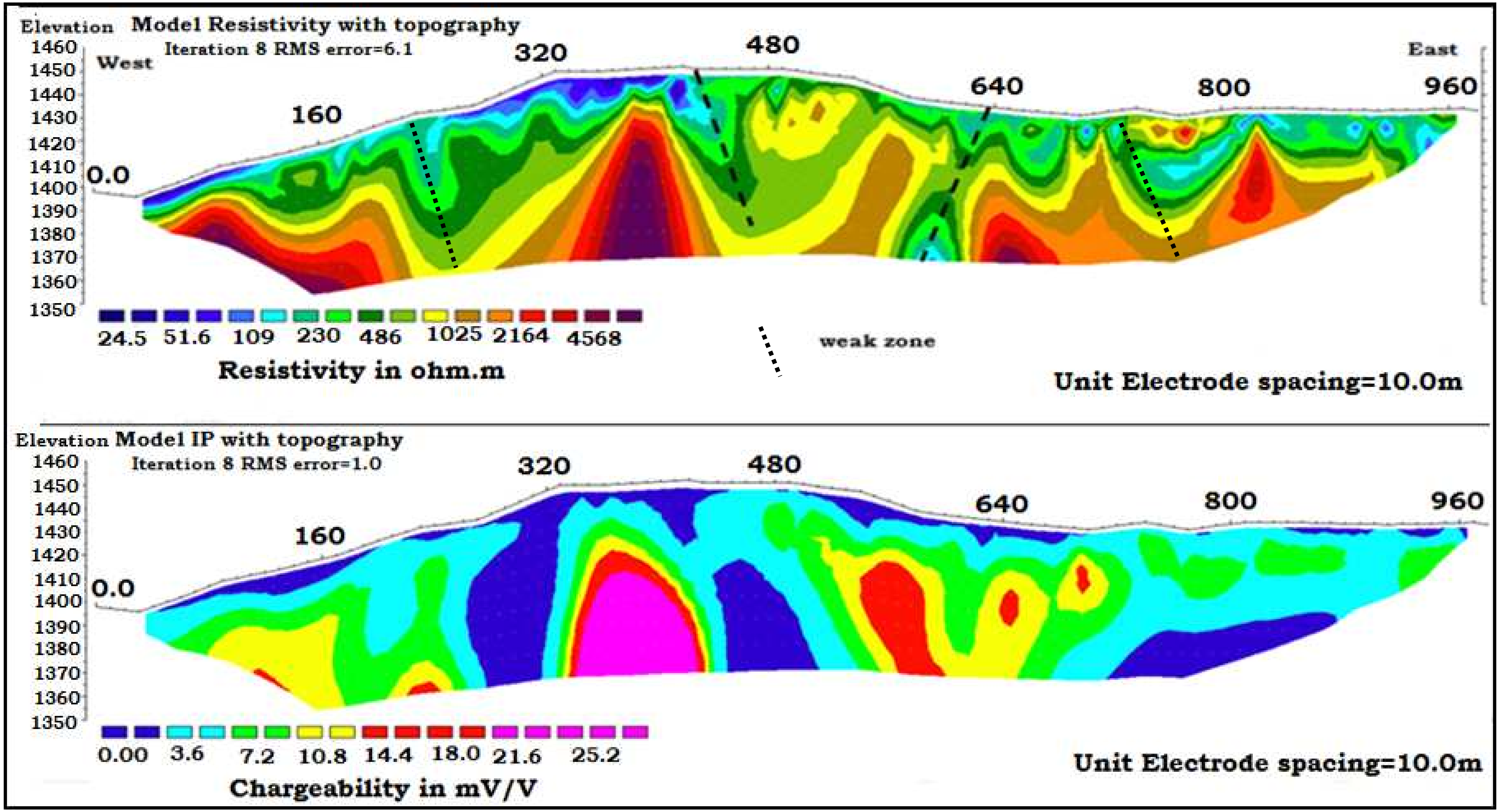

Figure 4.5 Inverse resistivity and chargeability model section of 800S

4.3.2 IP/Resistivity Inverse Model Section 600S

This profile runs for 890m laterally and 67.5m vertically, and like the previous line it also cuts dominantly through the orthogneisses, see figure 4.6. From the center of the line, the ground relief drops both sides with moderate slop.

The 2D resistivity inversion reveals at least three high resistive zones; the first one between 0m and 160m, then from 280m to 440m and the other between stations 640m and 760m.between stations 450m and 760m. At the surface of there appears a small pitches of higher resistivity at station 210m,390m and 780m. These resistivity highs correspond to the magnetic low of the analytical signal. These broad high resistive zones seem the response of granite gneisses, which is the dominant lithology of the study area.

In this profile, the chargeability inversion reveal only single high IP anomaly is detected between the station 650m and 750m. Its top emerges at a depth of about 35 meters, which is a contact zone between the orthogneisses with the amphibolite/minor metavolcanics in the eastern side. This anomaly possibly goes down to the larger depth and dips to the east.

The high IP anomaly in this profile also associated to the high resistivity and may be attributed to a sulphide mineralization zone hosted in intensively silicified horizon. This once again indicates the sulphide mineralization is fine grained and disseminated through the silicified zone rather than interconnected to each other.

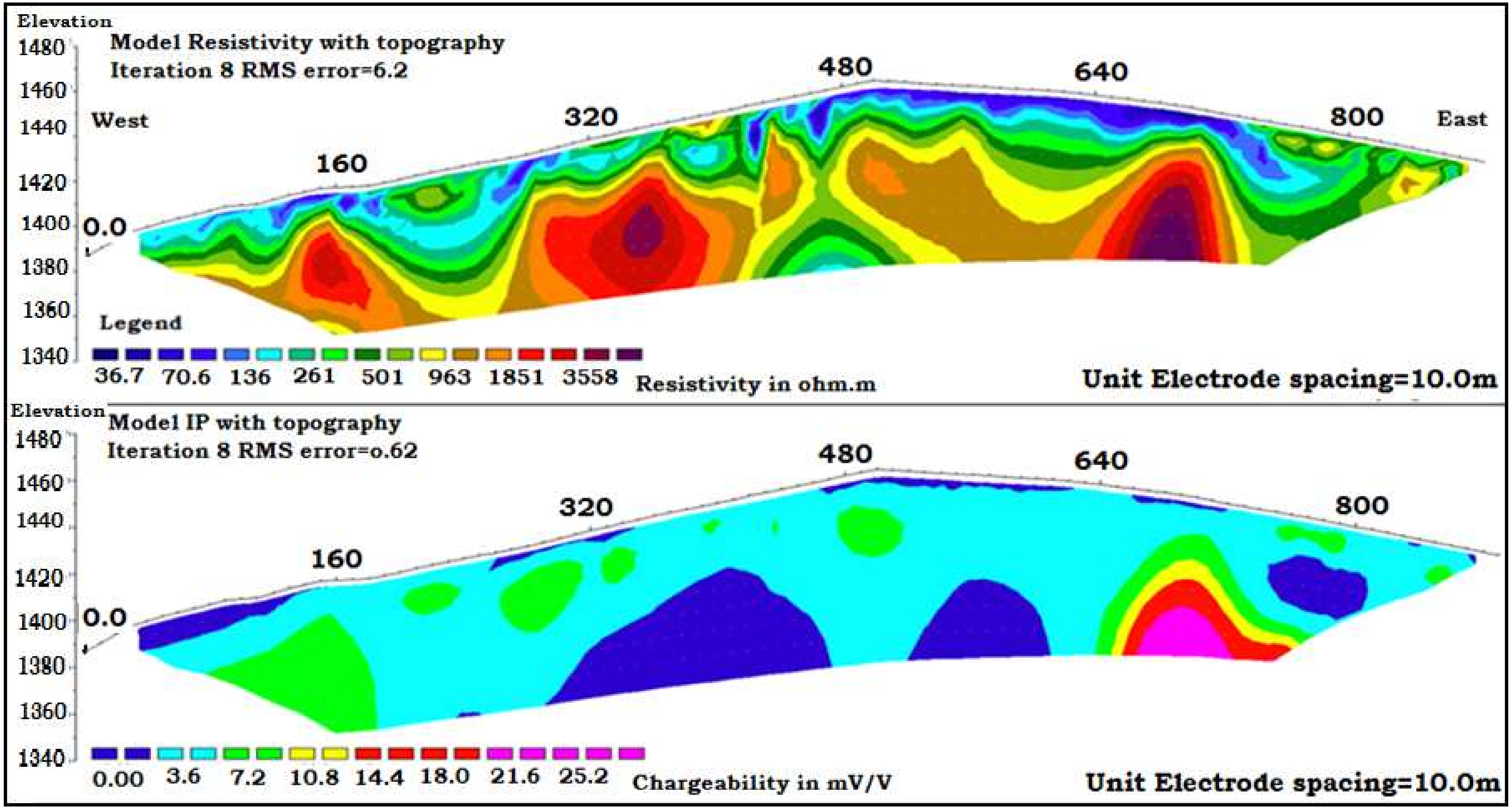

Figure 4.6 Inverse model resistivity and chargeability section 600S

4.3.3 IP/Resistivity Inverse Model Section 400S

This profile also covers a total distance of 890 meters horizontally and the inverted model showed that it went down to a depth of 67.5m as shown in the figure 4.7. Like the other profiles, this traverse also runs over the orthogenesis (deformed granitoids) and the amphibolite/minor metavolcanics. The subsurface elevation along this profile changes from 1360m, at the western side, to 1460m towards the eastern end.

The ground below this traverse line is covered by a relatively conductive (<90Ωm) materials of varying thickness. Within the thickest interval (330m-380m and 400m – 700m), the maximum depth of the conductive horizon reaches about 20m from the topographic surface. The formation resistivity gradually increases with depth and there appear three relatively high resistivity (>1000Ωm) dome-shaped bodies, at depth. The first one is detected at the stations between 0m and 180m. The second and third resistive bodies have their apexes at 320m and 640m, respectively. These two peaks seems to be parts of a vast single body in which the gap in between is filled with lower resistivity materials. Other two smaller resistive patches, likely signature of rock boulders, are mapped below stations 200m and 750m. The high resistivity zone, in this profile, also corresponds to moderate magnetic response of the area. The resistivity high and high IP may possibly be the response of the silicified horizon and disseminated mineralization.

The IP inversion result shows that very high single anomaly is found at the station 330m at a depth of about 58 meters and the other anomaly emerges and opens to the eastern end. Just like the other profiles, the high IP anomaly, in this profile, is also associated to the resistivity highs and lows, peaked at 320m.

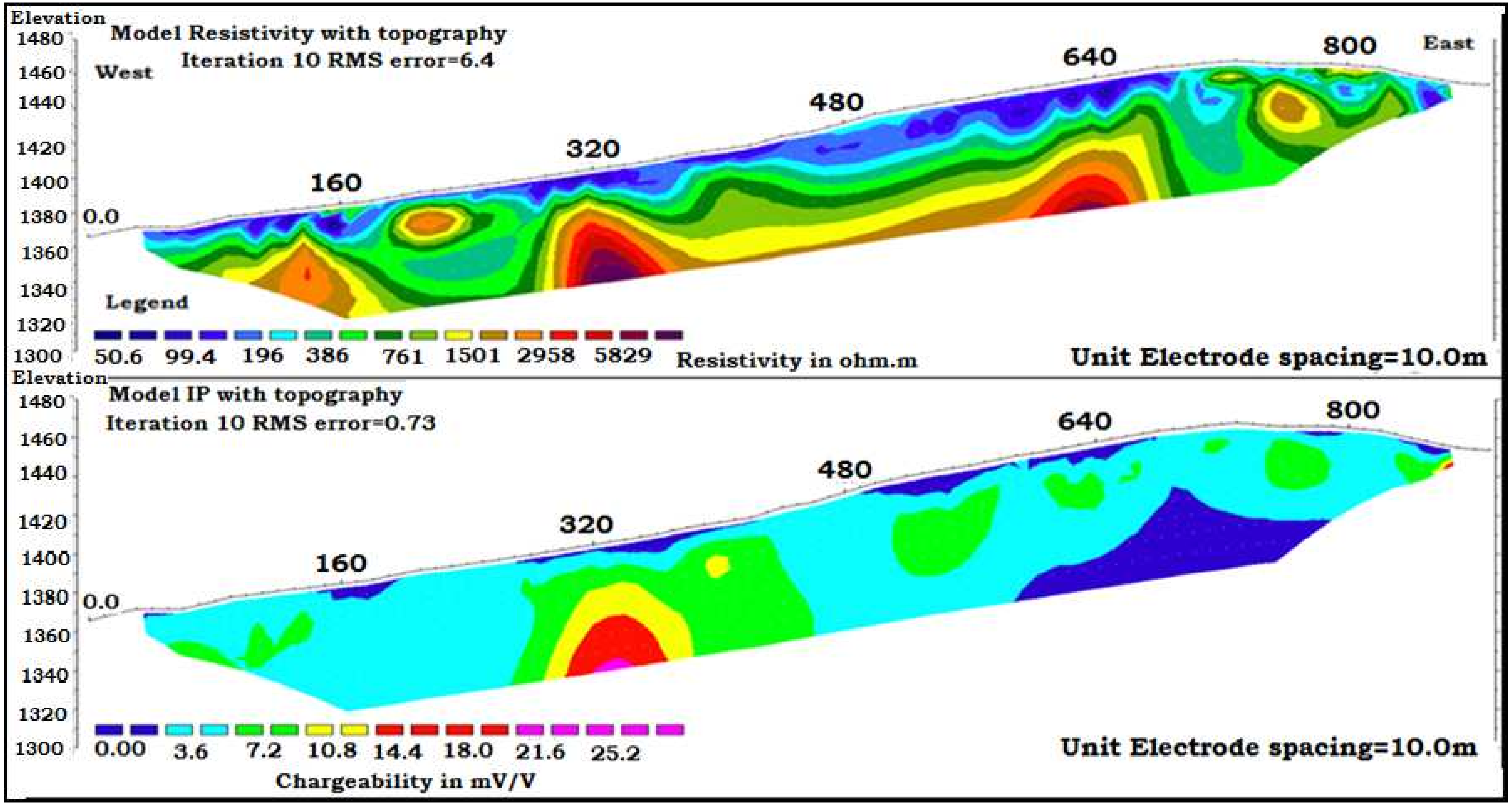

Figure 4.7 Inverse model resistivity and chargeability section of 400S

4.3.4 IP/Resistivity Inverse Model Section 200N

Line 200N is the longest profile covering a distance of about 1430m. It is also topographically disturbed, with localized hills and valleys, figure 4.8.

The 2D inversion result for this line reveals that a very strong subsurface electrical heterogeneity with numerous resistive bodies truncated by narrow conductive zones in a seemingly vertical banding. The most resistive bodies were encountered early on the profile, 0-400m with amplitude in excess of 3000Ωm is recorded and better IP anomalies are manifested. These high resistivities are between 0m and 570m, 640m and 780m, 800m and 900m, and 1120m and 1300m with conductive feature between them. From this profile, six weak zones are identified and marked by a dot lines, the four are trending NNW-SSE and the others area NNE-SSW in direction. Most high resistive, anomalies are corresponds to the magnetic high and moderate response of the analytic signal.

This profile cuts the amphibolite and minor metavolcanics and shows high resistive zone between the 300m and 580m. Several prominent IP anomalies are present on this profile. These anomalies are dispersed and not broaden to the deep except, the anomalies that are located at the station of 600m at a depth of about 54 meters and at station 1280m at a depth of 33 meters. Three very high IP anomalies are found between 270m and 340m, 410m and 480m,(which are shallow at a depth of about 22 meters) and below 600m and also smaller IP anomalies are located below 110m,510m,600m, 750m,880m, 1250m (broaden and dips to the east and may extends to depth), at 1400m. In this profile, the high IP is associated to the resistivity highs, except the anomalies between 510m and 640m, the association is low resistivity with high IP. In this profile, an exceptional higher IP anomaly is detected at 600m, which is manifested on the low resistive zone or on high conductive materials, indicates the sulphide mineralization is possibly hosted in quartz vein through the fracturing/sheared zone. However, the high IP anomalies, which are associated with the high resistivity, are possibly due sulphide mineralization with in quartzite in a disseminated manner. Since sericitization and epidotization occur around altered feldspar and chloritization around altered hornblende are observed at microscopic scale on the rock units of the area.

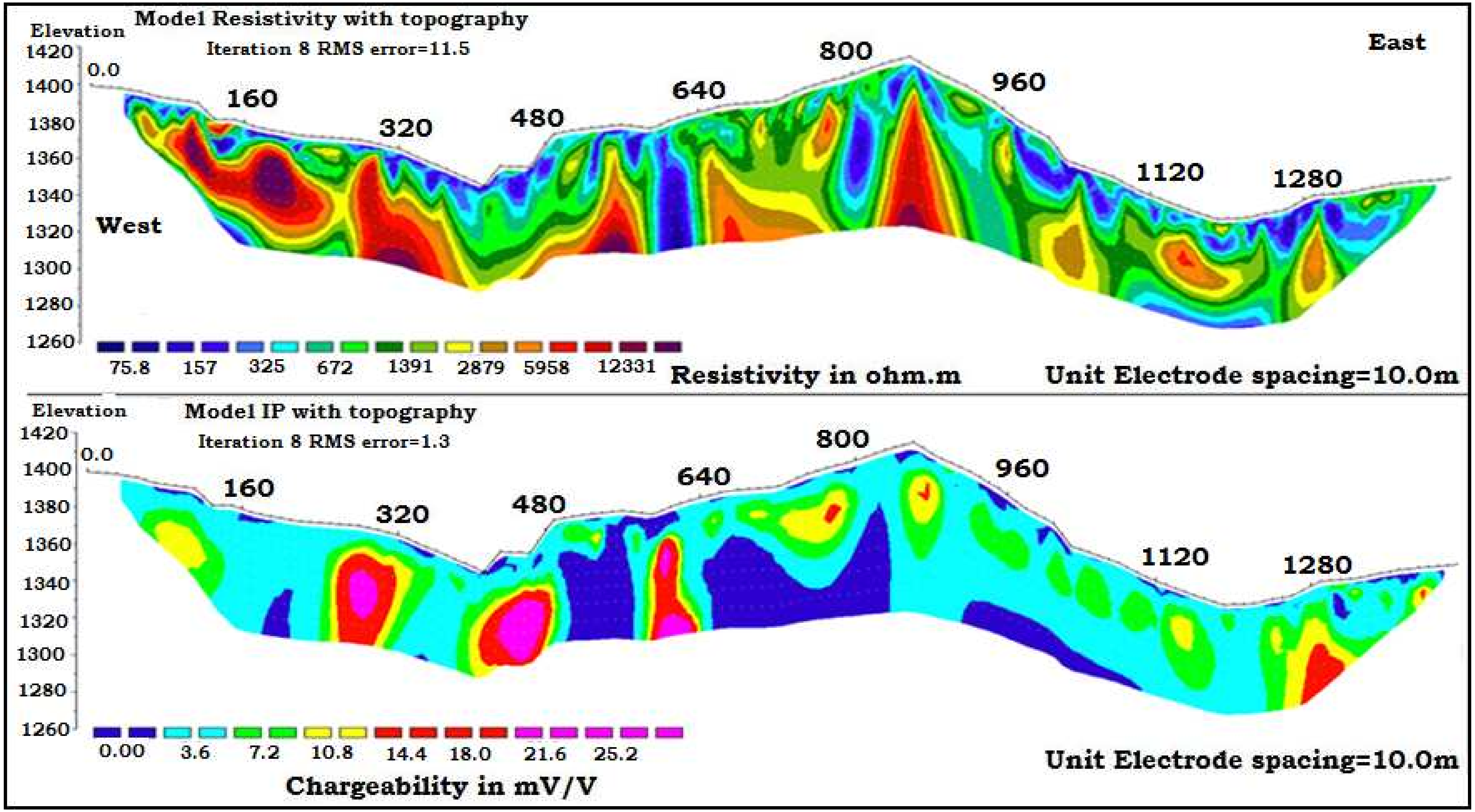

Figure 4.8 Inverse model resistivity and chargeability section of 200N

Moreover, the eastern end high IP anomaly on this profile exactly fits with the geochemical gold map (figure 2.4) and has an IP value between 14-18mV/V.

4.3.5 IP/Resistivity Inverse Model Section 800N

This profile is far 600m from the above profile figure 4.8. It covers a total horizontal distance of 620 meters and a vertical depth of 67.5m, figure 4.9. This profile also similar geological characterization to the other profiles i.e. orthogneisses and amphibolites. The subsurface elevation along this profile also changes from higher elevation 1460m, at the western side, to 1350m towards the eastern end. Moreover, the subsurface of this traverse covered by a varying thickness conductive material within the thickest interval at (500m-620m), the maximum depth of the conductive horizon reaches about 18m from the topographic surface.

The 2D inversion result of the resistivity tells conductive materials separate the high resistive zones. These high resistivities are situated between 0m and 310m, and 320m and 620m, and dips to west and east respectively. Additionally, the high resistive zones of this profile are corresponds to the magnetic high of the analytic signal. On the other hand, the conductive zone, which separates the high resistive zones, is also lies on the amphibolite and/or minor metavolcanics but due to shearing effect, the amphibolite schist moved to the west. This showed in this lithology high conductive materials are situated. It is located between 280m and 360m and with very low resistive material at greater depth.

Moreover, the 2D inversion result for the IP reveals a broad high IP anomaly to the western side of the profile in a continuous manner. This high IP anomaly has broadens to the western end. The occurrence of a few epidotes and sericites with slight alteration and medium to coarse-grained quartz characterize the amphibolite schists. Thus, the mineralization is possibly silicified quartz vein hosting and disseminated sulphide mineralization. Like the other profiles, on this profile also the high IP anomaly is associated with the resistivity highs.

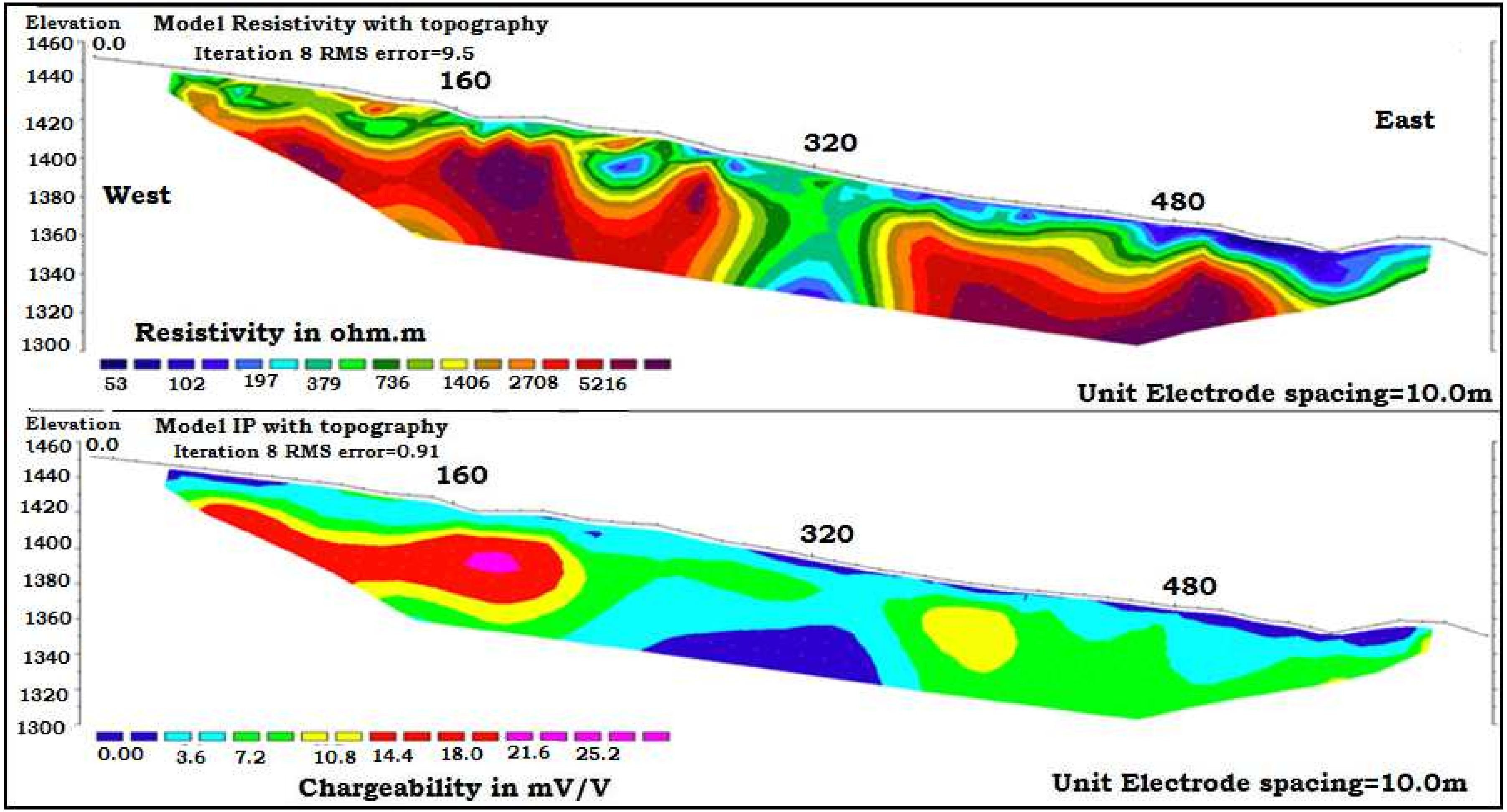

Figure 4.9 Inverse resistivity and chargeability section of 800N

4.3.6 IP/Resistivity Inverse model section 1200N

This is the last profile and covers 980m horizontally and 67.5m vertically and cuts the orthogneisses and amphibolite units, figure 4.10. The ground relief of this profile is also similar to the 800N profile but at the eastern end seems to increasing.

The resistivity inversion result reveals moderate to high resistivities and a high rugged signature are observed. Around the station 380m, the conductive feature showed going depth and separates the high resistive zones. The surface cover of this traverse showed entirely conductive materials within a varying thickness and maximum depth of the conductive horizon reaches about 20m at the western and 31m at the eastern side from the topographic surface, No high resistive boulder found at the surface of this profile. High resistivities are situated at stations 60m to 380m, 430m to 530m, 680m to 760m and 800m to 860m on this profile. 4730Ωm maximum and 33.3Ωm minimum resistivity values are recorded on this profile. On the other hand, moderate and high magnetic responses on the analytic signal map are detected on this profile. Moreover, east and west dipping high resistivity features are observed on the traverse and the high resistivities on the eastern side are slide to the south and east direction.

The IP inversion result reveals two prominent domed shaped IP anomalies. The first high IP is detected at the station 600m to 660m and its apex detected at a depth of about 30 meters and the second high IP anomaly also detected at the station 730m to 800m and emerges to a depth of about 58 meters. The high IP feature manifested on this traverse is on moderate resistivity zone. The second IP anomaly is lies on the amphibolite and minor meta-volcanics where as the first anomaly is the response of orthogenesis in the contact region. These highs showed possibly going to greater depth. On this profile, the high IP anomaly is associated with moderate and high resistivity of the inversion result. The high chargeability anomaly observed on the eastern lower level probably be due to sulphide minerals that are coated and intercalated with the high and moderate resistive zones from the amphibolite schist due to altered hornblende and intensively silicified wall rocks.

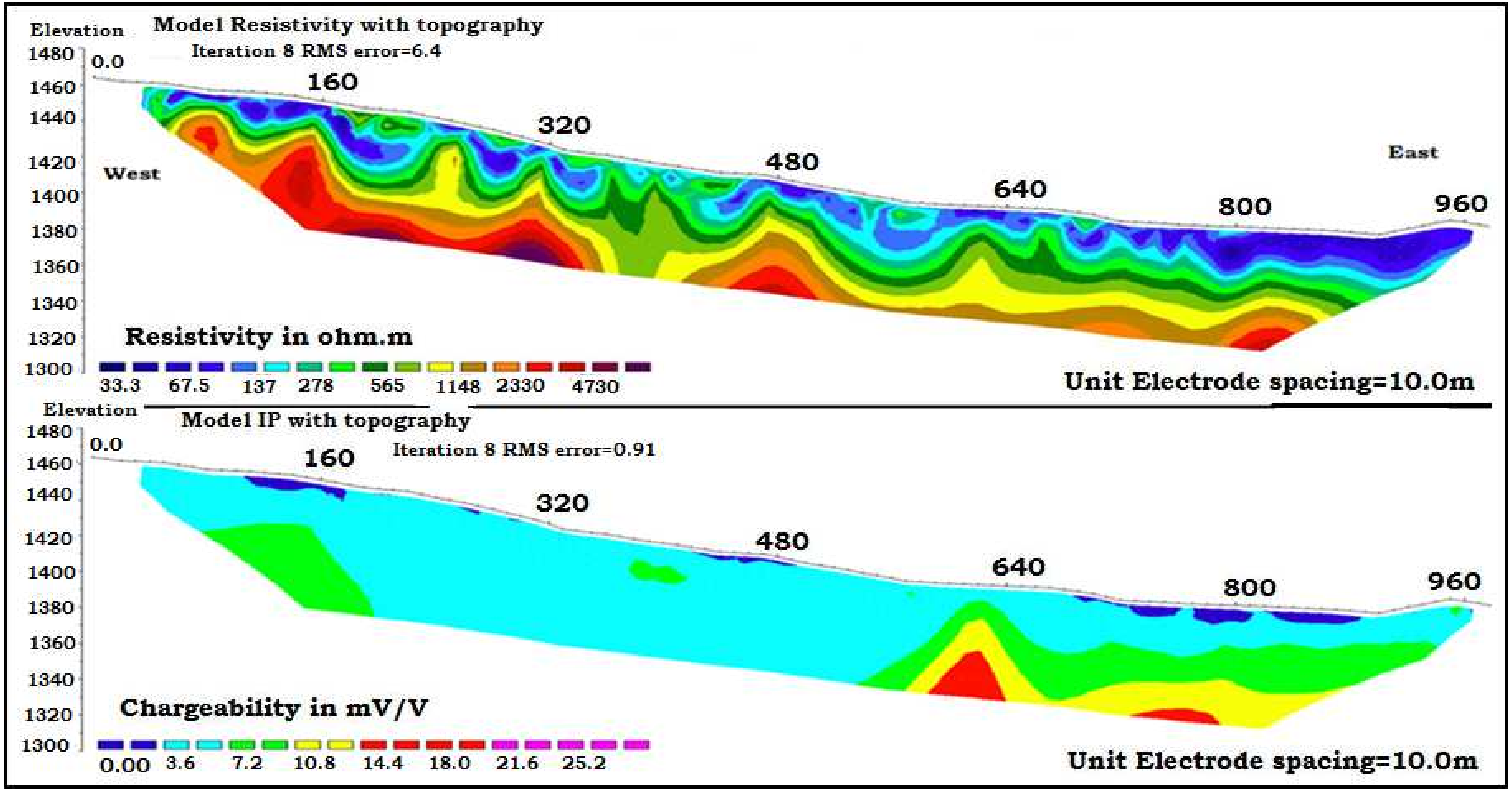

Figure 4.10 Inverse model resistivity and chargeability section of 1200N

4.4 Resistivity and Chargeability Sliced Stacked Depth Maps

The variation in resistivity and the chargeability of the study area as a whole is presented as a function of depth, showing the vertical as well as the horizontal variations with in the area. This resistivity and the chargeability values for different depths were extracted from RES2DINV output then exported to the Surfer format. It was finally processed and presented using Oasis montaj software. The brief discussion of the stacked section will be presented in reference to, figure 4.11 & 4.12.

For the purpose of interpretation, the resistivity and the chargeability values are grouped in to three. For the resistivity, the range 0-500 ohm-m, 500-1500-ohm-m and above 1500 ohm-m are designed as low, moderate and high respectively. In case of chargeability, 0-4mv/v as low, 4-10mv/v as moderate and above 10.4mv/v is labeled as high.

The stacked resistivity map interpretation (Figure 4.11)

On the top most slice, 13m depth, most of the area covered by low to moderate resistibility, but narrow patches of high resistivity are detected the central western and SSW flank. At the 26m depth, it has been shown that both the amplitude and lateral extent of the resistivity response increase. The western high resistivity in 13m extends to south and new high resistive zones are manifested at the flank of the NNW, a smaller at NNE, east and at the flank of SSW regions.

At depth of 39m, the northern part of the area is entirely covered by high resistivity response, trending E-W in direction. A smaller patch of higher resistivity also appears at SSW boarder. Moderate and low resistivity signatures cover the remaining part of the area. The new feature occurred at this depth is the WNW resistivity becomes narrow and extends to the SSW high resistive zone by forming NNE-SSW trending feature extending to the 53 meter depth map. Most of the features at 65m depth are similar to 53m depth picture, but the high resistivity zone in the northern part intensifies to NNE region of the area.

In conclusion, the stacked resistivity map of the area reveal that the amplitude of the north-western high resistivity zone increases with depth and trends to be oriented in NE-SW direction. The low resistivity response dominant at shallow depth, on the other hand, shows continuity from the surface to the depth with increasing signature at the SSE flank of the area

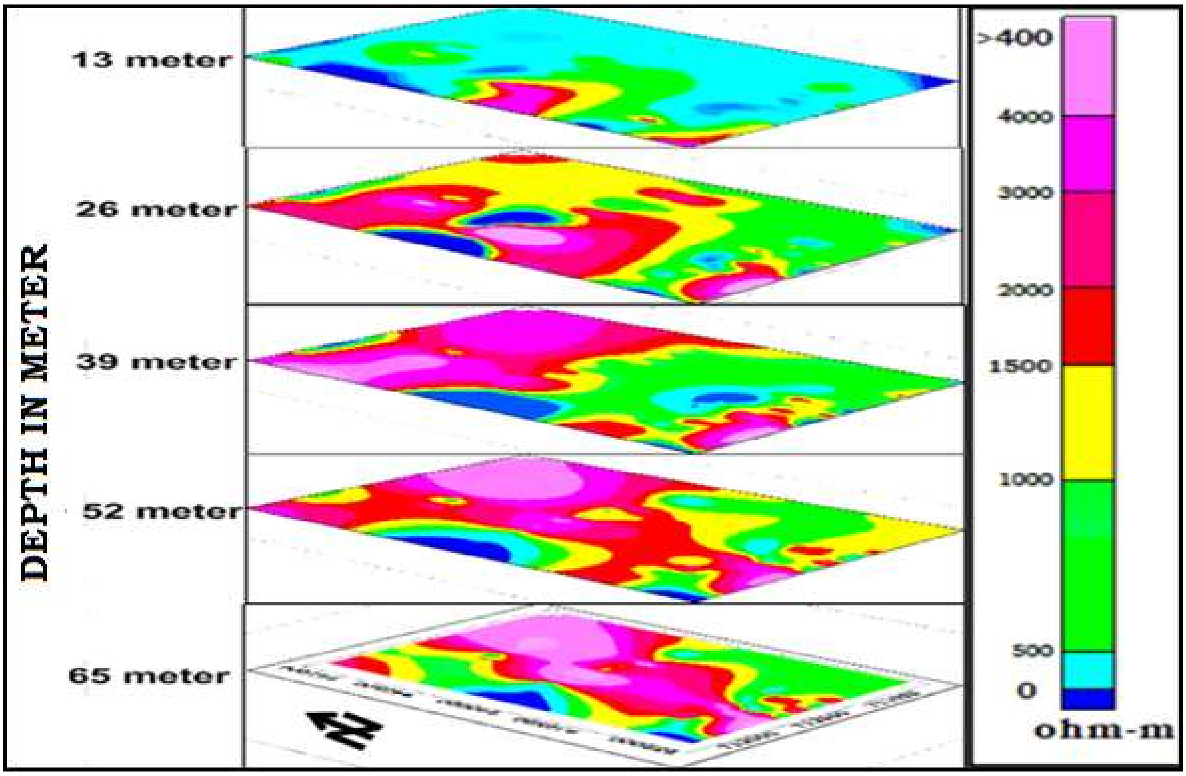

Figure 4.11 Stacked interpreted resistivity at different depth values

<u>The stacked chargeability map interpretation (Figure 4.12)</u>

Like the resistivity-stacked map, the stacked chargeability map has outlined prominent IP features on the grid.

At the 13m depth, most of the area is characterized by background response except a very narrow high IP zones manifested at the northern, central, and the eastern part of the area.

Down at 26m depth, the high IP zones detected at the NNW portion broadens both to the west and to south and tend to join the second high IP at the center of the area. But the smaller anomaly at the eastern flank seems to diminish. Other narrow anomaly area detected at southern border of the area.

On the 39m depth slice, the NNW IP anomaly extends to the SSE and connected to the central anomaly, which becomes narrow, the eastern anomaly in the 26m becomes wider and extends to the north and to the south. The SSW flank also show a change in magnitude and broaden to the east.

At 52m of depth, it is clearly observed that the central, NW trending anomaly tends to disappear and the eastern anomaly becomes broaden to the west and the south. The SSW flank remains the same or even narrower in extent.

The bottom, 65 meter depth map, shows the prominent high IP at the central eastern side gradually shifts to the south and other smaller anomalies emerge at the central portion and SSW corner of the area.

From the stacked sections, it is evident that, as the depth increases, the high IP anomaly shifts to the southeastern side of the area. This is at the contact of the granitic gneisses and the altered amphibolite. At shallower depths (up to 39m), most high IP anomalies are situated at western part but, beyond 39m depth, the high IP anomaly are strong on the eastern and SSE part of the area.

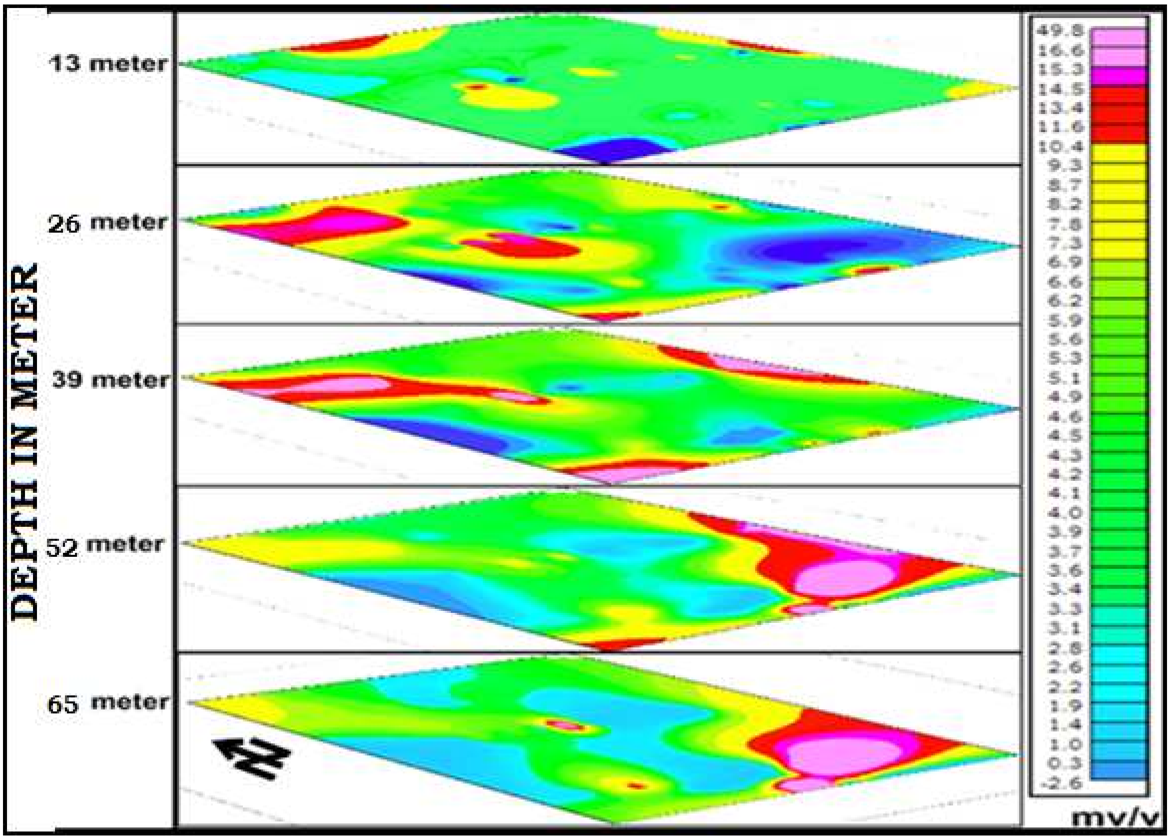

Figure 4.12 Stacked interpreted chargeability at different depths

CHAPTER FIVE

CONCLUTION AND RECOMMENDATION

5.1 CONCLUSIONS

IP/Resistivity and ground magnetic investigation are conducted in the study area, the following results are obtained.

- Ground magnetic signatures have been used to interpret the position of possible shear related structures. The magnetic analytic signal images are used to highlight these targets. These maps have identified position of magnetic minerals, showed maxima over the discrete bodies and prominent structures.
- Most of magnetic image results are correlated with the geologically mapped structures i.e. NNE-SSW and NNW-SSE (foliation, folding and shearing) and ESE-WNW and ENE-WSW fractures in the amphibole schist, the main host of mineralization, and also in the granitic gneiss.
- Highly magnetic susceptible minerals are outlined at the northern, northwestern and southeastern part of the area. It is correlated to the high gold anomaly revealed by geochemical result.
- The analytic signal and its first vertical and tilt derivatives also delineated NNE-SSW and NNW-SSE, E-W trending structures.
- Surface and subsurface structures (shear related fractures, fault zones and the general dip direction) have also been identified and overprinted by the Resistivity model section while mineralization is manifested on the IP model.
- The result of six IP/Resistivity model section reveal persistent very high response zones. These high resistivity anomalous zones are dipped mostly to the east and, unusually to the west and coincide to moderate to high IP responses.
- Prominent IP anomalies have been shown decreasing towards the west and increasing to the eastern side of the grid and its signature also intensifies going down to larger depths.
- More prominent IP zones, which can be attributed to mineralized zones, are detected in 200N and 800S profile maps than the other profiles.

- High IP anomalies are detected at the contact region of the amphibolite and also trends N-S in direction in the area. This conclusion is supported by the test trench geochemical results given in the EL Mining annual reports.
- High to moderate resistivity and very high magnetic signatures are detected over the silicified zones especially, at the eastern side of the area. These regions are characterized by medium to high IP response related to quartz vein hosted sulphide mineralization.
- The high resistivity response is attributed to intensive silicification or slight alteration of the rock while the intermediate to high chargeability is due to metallic sulphides or other conductive material hosted in intensively silicified wall rock.

Integrating the result of the current geophysical investigation to the previous geological and geochemical finding clearly identified a number of target area for further prospecting. Thus, the primary source of gold, in the study area, could be altered amphibolites schist hosting sulphidized quartz veins and veinlets. Hence, the possibly type mineralization expected in the area is thought to be disseminated and quartz vein hosted.

5.2 RECOMMENDATIONS

Based on the results obtained from the IP/Resistivity and the magnetic survey in the study area the following points are recommended.

- In addition to the IP/Resistivity and magnetic methods, using radiometric method in integration is advisable for better resolution of the alteration zone and lithologic units.
- The electrodes used in the current electrical IP/Resistivity were polarized electrodes, thus the flow of ions through an electrolyte (in this case, the soil) to an electrode results in the deposition of metallic and organic ions on the surface of the electrode. This ionic deposition will eventually create an electrically resistive layer, reducing or stopping the flow of electricity. This effect is known as 'resistance polarization'. Non-polarizing electrodes are designed to minimize this effect. So I recommend to being used non polarized electrodes (or pours pot with copper sulphate solution) with conventional IP.

- Due to limited length of the multi-electrode cables used for the 2D IP/Resistivity survey, the depth of investigation has been practically shallow, in the context of mineral exploration. Thus, in order to constrain the depth extent and obtain a better resolution on the geometry of the subsurface ore bodies, I recommend Titan24 system. It is effectively a combination of a pole-dipole and dipole-pole survey (i.e. simultaneously taking measurements on either side of the single transmitter electrode along the survey section) and has twice depth of investigation than also the convectional IP.

- After having done the above detail subsurface mapping, it might be worth to drill some of the coincident geochemical and geophysical anomalous zones.

- Based on the findings of current geophysical investigations, which are also supported by geological and geochemical surveys, the prominent anomalies attributed to the mineralized zone have been shown to be open to the eastern and southern border of the current detail area. Therefore, continuation along these directions is highly recommended.

Appendix I

Basic principles of (DC) Resistivity method

Electrical resistivity method

The resistivity method is an “active” method of geophysical exploration. It is based on the natural variation of the resistivities of rocks and minerals. The resistivities of rocks are largely determined by the properties of rocks, and by the concentration and salinity of the pore water.

The resistivity method is widely employed in mineral exploration, in mineral exploration; it can yield information on local geologic structure and lithology, and for the direct delineation of conducting mineralized zones simultaneously with the induced polarization (IP) method.

The purpose of electrical surveys is to determine the subsurface resistivity distribution by making measurements on the ground surface. From these measurements, the true resistivity of the subsurface can be estimated. The ground resistivity is related to various geological parameters such as the mineral and fluid content, porosity and degree of water saturation in the rock.

The fundamental physical law used in resistivity surveys is Ohm’s Law that governs the flow of current in the ground.

The equation; for Ohm’s Law in vector form for current flow in a continuous medium is given by

$$\boldsymbol{J} = \boldsymbol{\sigma E} \qquad \textbf{(1)}$$

Where σ is the conductivity of the medium, **J** is the current density and **E** is the electric field intensity.

In practice, what is measured is the electric field potential. We note that in geophysical surveys the medium resistivity ρ, which is equals to the reciprocal of the conductivity ($\rho=1/\sigma$), is more commonly used. The relationship between the electric potential and the field intensity is given by

$$\mathbf{E} = -\nabla\Phi \quad (2)$$

Combining equations (**1**) and (**2**), we get

$$\mathbf{J} = -\sigma\nabla\Phi \quad (3)$$

In almost all surveys, the current sources are in the form of point sources. In this case, over an elemental volume ΔV surrounding the a current source *I*, located at (x_s, y_s, z_s) the relationship between the current density and the current (Dey and Morrison 1979a) is given by

$$\nabla.\ \mathbf{J} = \left(\frac{I}{\Delta V}\right)\delta(x - x_S)\delta(y - y_s)\delta(z - z_s) \quad (4)$$

Where δ is the Dirac delta function. Equation (3) can then be rewritten as

$$-\nabla\cdot[\sigma(x,y,z)\nabla\phi(x,y,z)] = \left(\frac{I}{\Delta V}\right)\delta(x - x_S)\delta(y - y_s)\delta(z - z_s) \quad (5)$$

This basic equation gives the potential distribution in the ground due to a point current source.

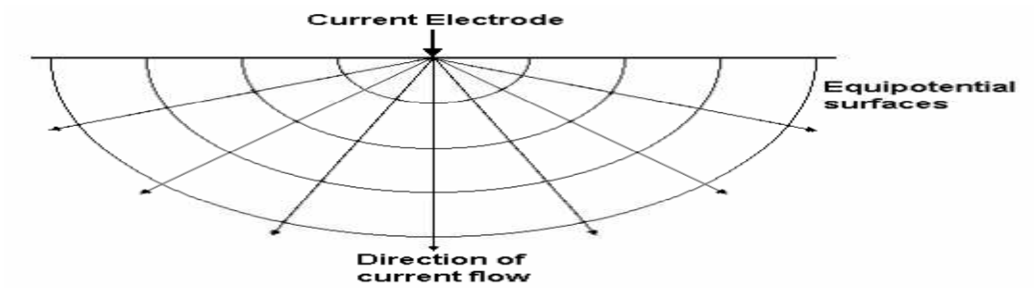

Figure 1*: The flow of current from a point current source and the resulting potential distribution.*

Consider a case with a homogeneous subsurface and a single point current source on the ground surface (Figure-1). In this case, the current flows radially away from the source, and the potential varies inversely with distance from the current source. The equipotential surfaces have a hemisphere shape, and the current flow is perpendicular to the equipotential surface. The potential in this case is given by

$$\phi = \frac{I\rho}{2\pi}\left(\frac{1}{r}\right) \quad (6)$$

Where r is the distance of a point in the medium (including the ground surface) from the electrode.

In practice, all resistivity surveys use at least two current electrodes, a positive current (source) and a negative current source (sink). The potential values have a symmetrical pattern about the vertical place at the mid-point between the two electrodes. The potential value in the medium from such a pair is given by

$$V_{p_1} = \frac{I\rho}{2\pi}\left(\frac{1}{r_{C1}} - \frac{1}{r_{C2}}\right) \quad \textbf{(7)}$$

Where r_{C1} and r_{C2} are distances of the point from the first and second current electrodes.

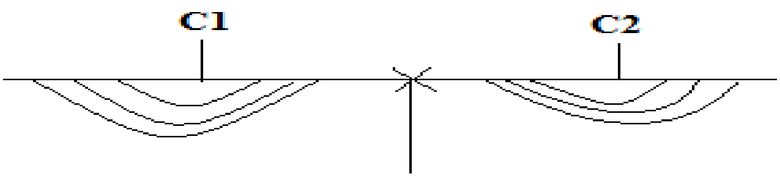

Figure 2: *The potential distribution caused by a pair of current electrodes a homogeneous half-space with resistivity* ρ.

In practically all surveys, the potential difference between two points (normally on the ground surface) is measured. A typical arrangement with four electrodes is shown in Figure 3.3. The potential difference is then given by

$$\Delta v = \frac{I\rho}{2\pi}\left[\frac{1}{r_{C1p1}} - \frac{1}{r_{C2p1}} - \frac{1}{r_{C3p2}} + \frac{1}{r_{C4p2}}\right] \quad \textbf{(8)}$$

The above equation gives the potential that would be measured over a homogenous half space with a four electrodes array.

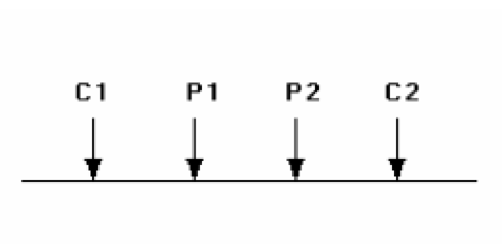

Figure 3: *A conventional arrays with four electrodes to measure the subsurface resistivity.*

Actual field surveys are invariably conducted over an inhomogeneous medium where the subsurface resistivity has 3-D distribution. The resistivity measurements are still made by injecting current into the ground through the two current electrodes (C1 and C2 in Figure 3.3), and measuring the resulting voltage difference at two potential electrodes (P1 and P2). From the current (I) and the potential (ΔØ) values, an apparent resistivity ((ρ_α) value is calculated.

$$\boldsymbol{\rho_\alpha = K\left(\frac{\Delta\emptyset}{I}\right)} \tag{9}$$

Where $\mathbf{K} = \frac{\mathbf{2\Pi}}{\left[\frac{1}{r_{C1p1}} - \frac{1}{r_{C2p1}} - \frac{1}{r_{C3p2}} + \frac{1}{r_{C4p2}}\right]}$

K is a geometric factor that depends on the arrangement of the four electrodes. Resistivity measuring instruments normally give a resistance value, $\boldsymbol{R} = \Delta\emptyset/\mathbf{I}$, so in practice the apparent resistivity value is calculated by

$$\boldsymbol{\rho_\alpha} = \mathbf{K}\boldsymbol{R} \tag{10}$$

The calculated resistivity value is not the true resistivity of the subsurface, but an "apparent" value that is the resistivity of a homogeneous ground that will give the same resistance value for the same electrode arrangement.

Common Electrode Arrangements in Resistivity Survey

Different electrode arrangement (configuration) have been applied in electrical survey to measure apparent resistivity of rock materials which are Wenner (alpha, beta, and gamma), Shelumberger, dipole-dipole, pole-dipole, pole-pole, Wenner-Shelumberger, Equatorial dipole-dipole.

Only Wenner-Shelumberger and dipole-dipole arrays are applied in the present study thus, we focus on these methods.

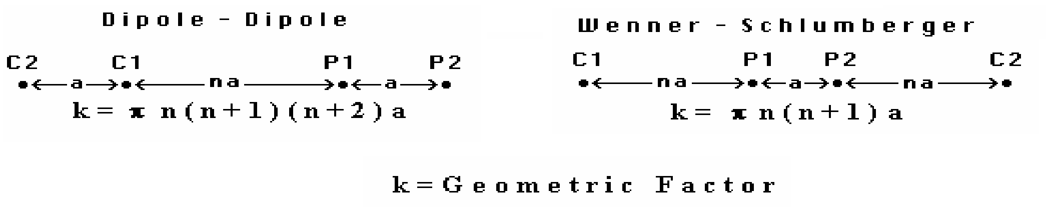

Figure 4: *Dipole-dipole and Wenner-Shelumberger arrays.*

A. The Dipole-Dipole array

This array has been, and is still, widely used in resistivity and IP surveys because of the low EM coupling between the current and potential circuits.

It is one of the families of arrays using dipole (closely spaced electrode pairs) to measure the curvature of the potential field. It has an arrangement such that the current electrodes are the same distance apart as the potential electrodes ($\boldsymbol{a}$) and they are separated from each other by a much greater distance ($\boldsymbol{na}$, where $\boldsymbol{n}$ is the dipole separation factor and $\boldsymbol{a}$ is dipole length), figure-4 of above.

If the separation between both pairs of electrodes is the same$a$, and the centers of the dipole is restricted to *a (n+1)*, the apparent resistivity is given by

$$\boldsymbol{\rho_\alpha = \pi n(n+1)(n+2)a\left[\frac{\Delta V}{I}\right]} \qquad \textbf{(11)}$$

The dipole-dipole array is very sensitive to horizontal changes in resistivity, but relatively insensitive to vertical changes in the resistivity. That means that it is good in mapping vertical structures, such as dykes and cavities, but relatively poor in mapping horizontal structures such as sills or sedimentary layers. The median depth of investigation of this array depends on both the "**a**" spacing and the "**n**" factor). In general, this array has a shallower depth of investigation compared to the Wenner array.

The dipole-dipole array might be a more suitable choice if good horizontal resolution and data coverage is important (assuming your resistivity meter is sufficiently sensitive and there is good ground contact).

B. Wenner-Shelumberger Array

This is a new hybrid between the Wenner and Schlumberger arrays (Pazdirek and Blaha, 1996) arising out of relatively recent work with electrical imaging surveys. The classical Schlumberger array is one of the most commonly used arrays for resistivity sounding surveys. This array might be a good compromise between the Wenner and the dipole-dipole array. The median depth of investigation for this array is about 10% larger than that for the Wenner array for the same distance between the outer (C1 and C2) electrodes, for "**n>3**" values.

It is a type of configuration, the potential electrodes are between the current electrodes, but the distance between them is (a) considerably less than or equal to the distance between the current electrodes (*na*), figure-4 of above. If the separation between potential electrodes is (*a*) and current electrodes (*na*), the apparent resistivity is given by

$$\rho_\alpha = \Pi n(n+1)a\left[\frac{\Delta V}{I}\right] \qquad \textbf{(12)}$$

The Wenner-Schlumberger array (with overlapping data levels) is a reasonable all-round alternative if both good and vertical resolutions are needed, particularly if good signal strength is also required.

Electrical Properties of Earth Materials

Electrical current flows in earth materials at shallow depths through two main methods. They are electronic conduction and electrolytic conduction. In electronic conduction, the current flow is via free electrons, such as in metals. In electrolytic conduction, the current flow is via the movement of ions in ground water. In environmental and engineering surveys, electrolytic conduction is probably the most common mechanism. Electronic conduction is important when conductive minerals are present, such metal sulphides and graphite in mineral surveys.

The resistivity of common rocks, soil materials and chemicals (Keller and Frischknecht 1966, Daniels and Alberty 1966, Telford et al.1990), Igneous and metamorphic rocks typically have high resistivity values. The resistivity of these rocks is greatly depends on the degree of fracturing, and the percentage of fractures filled with ground water. Thus a given rock type can have a large range of resistivity, from about 1000 to million ohm, depending on whether it is wet or dry. This characteristic is useful in the detection of fracture zone and other weathering features, such as in engineering and ground water survey.

The resistivity of several types of ores are different especially metallic sulphides (such as pyrrhotite, galena and pyrite) have typically low resistivity values of less than 1 ohm. Note that the resistivity value of a particular ore body can differ greatly from the resistivity of the individual crystal. Other factors, such as the nature of the ore body (massive or disseminated) have a significant effect. Note that graphitic slates have a low resistivity value, similar to the metallic sulphides, which can give rise to a problem in mineral survey. Most oxides, such as hematite, do not have a significantly low resistivity value. One of exception is magnetite.

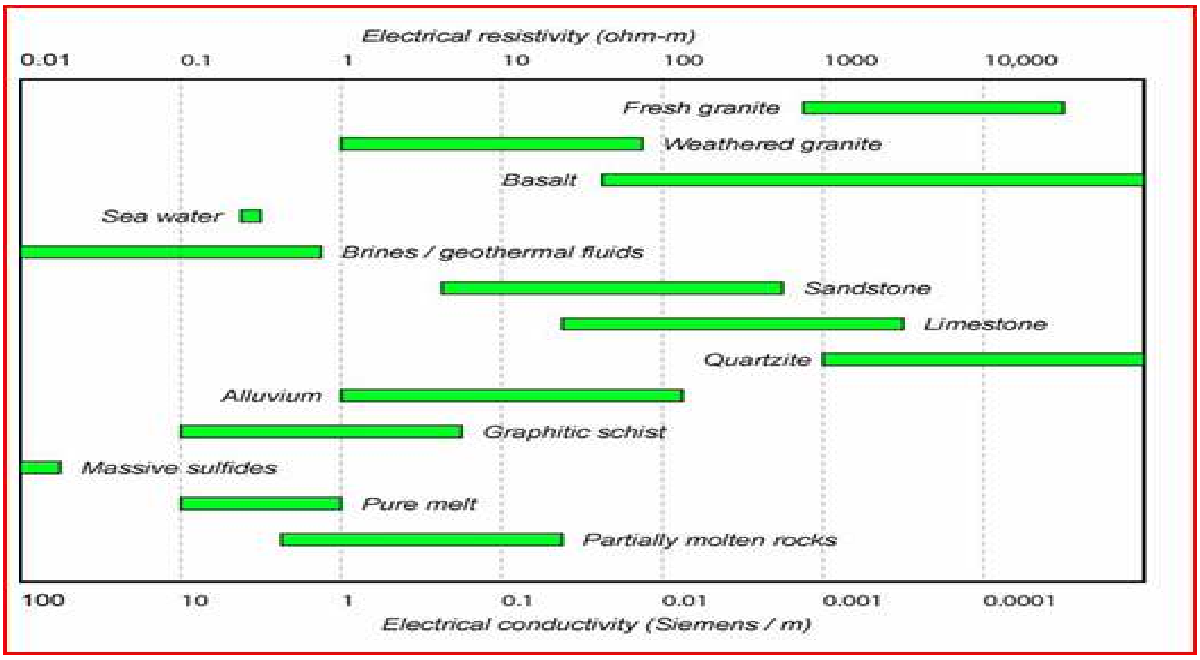

Figure 5: *Resistivity of most rock minerals.*

Field Procedures

There are two basic field procedures, which are used in resistivity surveying: SOUNDING and PROFILING.

- Resistivity sounding is essentially a depth investigation, and is an attempt to determine the variation of resistivities of the earth as a function of depth. This procedure is sometimes is called vertical electrical sounding (VES) or vertical profiling. The arrays used are Wenner, Shelumberger and the dipole- dipole arrays.

- Resistivity profiling is employed for lateral investigations, and is attempting to determine the variation of resistivities in the horizontal direction. The interpretation of resistivity profiling data is mostly qualitative, and consists of delineating zones of anomalously low or high resistivities (relative to the general background resistivity).

In mineral exploration, zones of low resistivities which might be correlatable with conductive (e.g. sulphide) mineralization are interesting.

For the dipole-dipole and Wenner-Schlumberger arrays (Figure-4), the survey procedure is slightly different. The distance between the current dipole and the potential dipole is increased in steps, as an example, for the dipole-dipole array, the measurement usually starts with a spacing of "**1a**" between the C1-C2 (and also the P1-P2) electrodes. The first sequence of measurements is made with a value of 1 for the "**n**" factor (which is the ratio of the distance between the C1-P1 electrodes to the C1-C2 dipole length), followed by "**n**" equals to 2 while keeping the C1-C2 dipole pair spacing fixed at "**1a**". When "**n**" is equals to 2, the distance of the C1 electrode from the P1 electrode is twice the C1-C2 dipole length. For subsequent measurements, the "**n**" spacing factor is usually increased to a maximum value of about 6, after which accurate measurements of the potential are difficult due to very low potential values. To increase the depth of investigation, the spacing between the C1-C2 dipole pair is increased to "**2a**", and another series of measurements with different values of "**n**" is made. If necessary, this can be repeated with larger values of the spacing of the C1-C2 (and P1-P2) dipole pairs. A similar survey technique can be used for the Wenner-Schlumberger array where different combinations of the "**a**" spacing and "**n**" factor can be used.

One technique used to extend horizontally the area covered by the survey, particularly for a system with a limited number of electrodes, is the roll-along method. After completing the sequence of measurements, the cable is moved past one end of the line by several unit electrode spacings. All the measurements that involve the electrodes on part of the cable that do not overlap the original end of the survey line are repeated.

APPENDIX II

Induced Polarization Method

Induced polarization (IP) is a relatively new technique in geophysics, and has been employed mainly in base-metal exploration and to a minor extent in groundwater search. Although the Schlumberger brothers, the great pioneers in geophysical exploration, had recognized the phenomenon of induced polarization some 60 years ago, during their original work in self-potential, its popularity as a geophysical tool dates from the mid-1950s, following further development work from 1948 to 1953. One form of polarization, the overvoltage effect, has been familiar in the field of physical chemistry for an even longer time (Telford, et al, 1996).

The induced polarization method provides a measure of polarizable minerals (metallic-luster sulfide minerals and clays,) within water-bearing pore spaces of rocks. Polarizable minerals, in order to be detected, must present an active surface to pore water. Because induced polarization responses relate to active surface areas within rocks, disseminated sulfide minerals provide a much better target for this method than massive sulfide deposits, although in practice most massive sulfide deposits have significant gangue and have measurable induced polarization. Induced polarization has found its greatest application in exploration for disseminated sulfide ore, where it may detect as little as 0.5 volume percent total metallic luster sulfide minerals (Sumner, 1976).

Origin of Induced Polarization

The exact causes of induced polarization are still unclear but most probably, induced polarization results from the combined effects of several physical chemical processes. However, two main mechanisms are reasonably understood: the membrane polarization and the electrode polarization effects. The membrane polarization effect is largely caused by clay minerals present in the rock or sediment. This is particularly relevant in engineering and environmental surveys. Conductive minerals in rocks cause the electrode polarization effect such that the current flow is partly electrolytic (through groundwater) and partly electronic (through the conductive mineral). This effect is of particular interest in surveys for metallic minerals, such as disseminated sulfides.

The induced polarization effect opposes the build up and collapse of the primary potential difference, and is referred to as the *overvoltage* because an extra voltage above that required to overcome the ohmic resistance is required to drive current through the ore zone. High porosity and high groundwater conductivity reduce IP as both lead to a short-circuiting of energizing current through unblocked paths (Griffiths and King, 1965).

Foremost among the ore mineral having an electronic mode of conduction and therefore exhibiting strong IP are pyrite, pyrrhotite, chalcopyrite, graphite, galena, bornite, magnetite and pyrolusite.

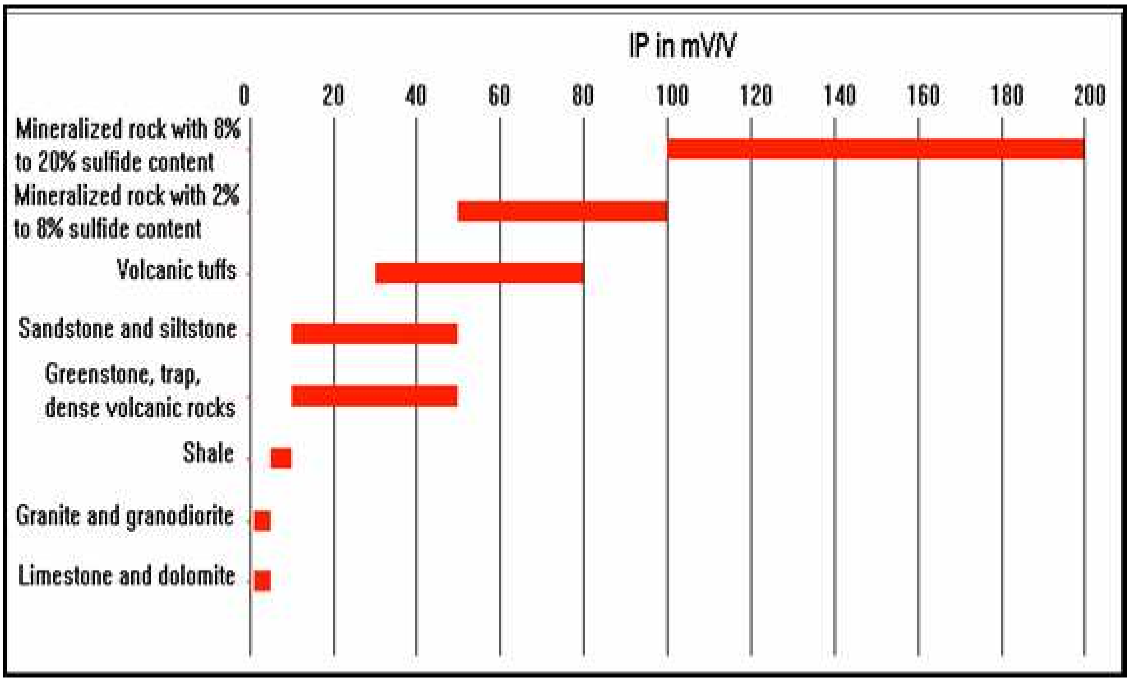

Figure 6: *The IP values for some rocks and minerals.*

Methods of Measurement of IP Effect

An IP measurement is made in the time-domain or frequency domain. In the time domain, the IP effect is measured by the residual decay voltage after the current is switched off. The time domain IP unit, the chargeability, is usually given in milivolt per volt (mV/V) or in milliseconds. Figure 3.6 shows the IP values (in terms of mV/V) for several mineralized rocks and common rocks. Note that the IP effect due to sulfide mineralization (the electrode polarization effect) is much larger than that due to clay minerals (membrane polarization) in sandstone and siltstones.

In the frequency domain, it is measured by the change in apparent resistivity value from low to high frequencies (typically 1 to 10 Hz) where the unit used is the percent frequency effect. Another measure of the IP effect in the frequency domain is the phase shift between the potential signal and the input current, where the unit used is in milli-radians.

IP Data Types

Although the chargeability is defined as the ratio of amplitude of the residual voltage to the DC potential immediately after the current cut-off, this is not used in actual field measurements. Field measurements of the IP effect may be divided into two main groups, the time-domain and frequency domain (not necessary mention here) methods.

Time Domain IP Measurements

In the time-domain method, the residual voltage after the current cut-off is measured. Some instruments measure the amplitude of the residual voltage at discrete time intervals after the current cut-off. A common method is to integrate the voltage electronically for a standard time interval. In the Newmont M_{331}standard (Van Voorhis *et al.* 1973), the chargeability, m_t is defined as

$$\boldsymbol{m_t = 1870\frac{\int_{0.15}^{1.1} V_S dt}{V_{DC}}} \qquad \textbf{(13)}$$

Where the integration is carried out from 0.15 to 1.1 seconds after the current cut-off. The chargeability value is given in milliseconds. The chargeability value obtained by this method is calibrated (summer, 1976) so that the chargeability value in msec has the same numerical value as the chargeability given in mV/V. In theory, the chargeability in mV/V has a maximum possible value of 1000. Frequency domain IP is not implemented on this research.

The techniques of sounding and profiling used in the resistivity measurements are also used in IP method.

APPENDIX III

Magnetic Survey Method

The magnetic method of geophysical prospecting is a passive potential method of geophysical exploration. It is based upon the variation of the earth`s magnetic field caused by variation in the magnetization of rocks. To a large extent these variations reflect the magnetite content of the rocks, but magnetic anomalies are also caused by other magnetic minerals such as Pyrrhotite.

Magnetic prospective is the oldest and the cheapest of the geophysical method used to explore both oil and mineral. Thus, it is commonly possible to estimate the depth of basement and under favourable circumstances, quantitatively map basement structures, such as faults and horst rocks (Parasins, 1975).

In mining exploration, the magnetic methods have been employed chiefly in the search of magnetic minerals, like magnetite, chromites and pyrrhotite. Magnetics are routinely used to search for hydrothermal alteration in association with porphyry systems, and can be used to map buried stream channels (magnetite sands) that might host placer gold.

There for, the method is very effective to determine the depth, size or structure of mineralized zones for which there is no surface evidence because of alluvial or vegetative cover.

Fundamental Principle of Magnetic Method

Magnetic Force

The mathematical expression for the magnetic force, F, experienced between two magnetic poles of strength m_1 *and* m_2 separated by a distance r is obtained from Cloumb's law and is given by

$$\mathbf{F} = \frac{(\mathbf{m_1 m_2})}{\mu \mathbf{r^2}} \quad \mathbf{(14)}$$

The constant μ known as ***the magnetic permeability,*** is a property of the material in which the two monopoles, m_1 and m_2 are located. If they are in a vacuum, μ is called the magnetic permeability of free space. It depends up on the magnetic properties of the medium in which the poles are situated.

A more practical quantity than the force is the magnetic field strength (H) existing at a point in space, as a result of a pole of strength m located at a distance r from it. It is defined as the force per unit pole.

$$\mathbf{H} = \frac{\mathbf{F}}{\mathbf{m'}} = \left(\frac{\mathbf{m}}{\mathbf{\mu r^2}}\right) \qquad \mathbf{(15)}$$

Since isolated pole do not exist, actual magnets are generally considered to be magnetic dipoles. A dipole consist of two poles of equal strength m and of opposite sign separated by a short distance L. Then a magnetic moment (m) is given by

$$\mathbf{M} = \mathbf{mL} \qquad \mathbf{(16)}$$

The magnetic moment is a vector in the direction of a unit vector extending from the negative pole towards the positive pole.

Magnetic Susceptibility

When a magnetic material is placed within a magnetic field strength, *H*, the magnetic material will produce its own magnetization. This phenomenon is called *induced magnetization*. In practice, the induced magnetic field will look like it is being created by a series of magnetic dipoles located within the magnetic material and oriented parallel to the direction of the inducing field, *H*. The strength of the magnetic field induced by the magnetic material due to the inducing field is called the intensity of magnetization, I.

The intensity of magnetization defined as the dipole moment per unit volume V of a material, given by

$$\mathbf{I} = \frac{\mathbf{M}}{\mathbf{V}} \qquad \mathbf{(17)}$$

The intensity of magnetization, *I*, is related to the strength of the inducing Magnetic field, *H*, through a constant of proportionality, *k*, known as the Magnetic Susceptibility, which is a measure of how susceptible a material is to becoming magnetized.

$$\mathbf{K} = \frac{\mathbf{I}}{\mathbf{H}} \quad \textbf{(18)}$$

The magnetic susceptibility is a unit less constant that is determined by the physical properties of the magnetic material. It can take on either positive or negative values. Positive values imply that the induced magnetic field, *I*, is in the same direction as the inducing field, *H*. Negative values imply that the induced magnetic field is in the opposite direction as the inducing field.

In magnetic prospecting, the susceptibility is the fundamental material property whose spatial distribution we are attempting to determine. In this sense, magnetic susceptibility is analogous to density in gravity surveying.

The magnetic response of rocks and minerals is determined by the amount of magnetic material (magnetite) in them. It is very small for most natural materials, and may be either negative (diamagnetism). Sediments and acidic igneous rocks have small susceptibilities whereas basalts, dolerites, gabbros and serpentinites are usually strongly magnetic. Weathering generally reduces susceptibility because magnetite oxidized to hematite but some laterites are magnetic because of the presence of magnetite and remanently magnetized hematite.

Magnetic Induction

The ratio of the flux density **B** (also called *magnetic induction*) to the magnetizing field strength H is a constant called the *absolute magnetic permeability* (μ). Practically, the magnetic permeability of water and air can be taken to be equal to the magnetic permeability of free space (vacuum), denoted byμ_o which has the value of $4x10^7\,Wb\ /\ Am$. For any medium other than a vacuum, the ratio of the permeabilities of a medium to that of free space is equal to the *relative permeability* μ_r, such that $\boldsymbol{\mu_r} = \frac{\boldsymbol{\mu}}{\boldsymbol{\mu_o}}$ and, as it is a ratio, it has no unit.

$$\boldsymbol{B = \mu H} \quad \textbf{(19)}$$

Since $\boldsymbol{\mu = \mu_r \mu_o}$the above equation be comes

$$\boldsymbol{B = \mu_r \mu_o H} \quad \textbf{(20)}$$

Rearranging to introduce $\boldsymbol{k = \mu_r - 1}$ and we have

$$B = \mu_O H + \mu_O KH = \mu_O (H + I) \quad \textbf{(21)}$$

Where H and I are in the same direction, as is usually the case. The SI unit for **B** is the tesla=1newton/ampere-meter= 1weber/meter^2 (Wb/m^2). In vacuum $\mu_r = 1$ and in air $\mu_o = 1$. In magnetic prospecting, we measure **B** to about 10^{-4} of the earth's main field. The unit of magnetic induction generally used for geophysical work in the nanotesla (also called the gamma,γ) in which$1\gamma = 10^{-9}T = 1nT$.

The Earth`s Magnetic Field

The earth's magnetic field consists of three components: 1) the main field, 2) the external field and 3) magnetizable materials within the earth's crust. The main field, which accounts for over 99% of the earth's total magnetic field is internal in origin and is thought to be caused by convection currents of conducting material (mainly iron and nickel) within the liquid outer core. The earth's main magnetic field approximates to a first degree a magnetic dipole and is the inducing field for magnetizable objects within the earth's crust. The main field consists of several magnetic elements. These elements include: 1) magnitude of the field (F), 2) magnetic inclination (I) which is the dip of a magnetic compass needle from horizontal (e.g., magnetic south pole is -90^0, magnetic north pole is 90^0, and magnetic equator is 0^0), and 3) magnetic declination (D) which is the angle between geographic and magnetic north. Figure 7 shows the relationship between these values. These values are collectively known as the International Geomagnetic Reference Field (IGRF).

Additionally, the earth's main magnetic field changes with time due to variations in the motion of the convection currents within the outer core. These changes (called westward drift or secular variations) cause the magnitude, inclination and declination to change with time. As a consequence, the IGRF is updated every ten years or so and is revised to give the DGRF (Definitive), which is current reference model of the earth's magnetic field.

The external magnetic field (also called diurnal variations) is due to electric currents within the earth's ionosphere. These currents are mainly caused by interactions with plasmas connected with solar winds. These diurnal variations fluctuate rapidly but smoothly with time (minutes to hours) with maximum amplitudes varying from 50 to 200 gammas. On some days, these fluctuations are more random with amplitudes of several hundred gammas and are called magnetic storms. These storms are associated with solar flares and sunspot activity, and may persist for hours or several days. During such storms, magnetic surveying should be stopped.

The magnetizable materials within the earth's crust create small amplitude magnetic fields that cause spatial variations of the earth's main magnetic field. These materials are the targets of the magnetic method.

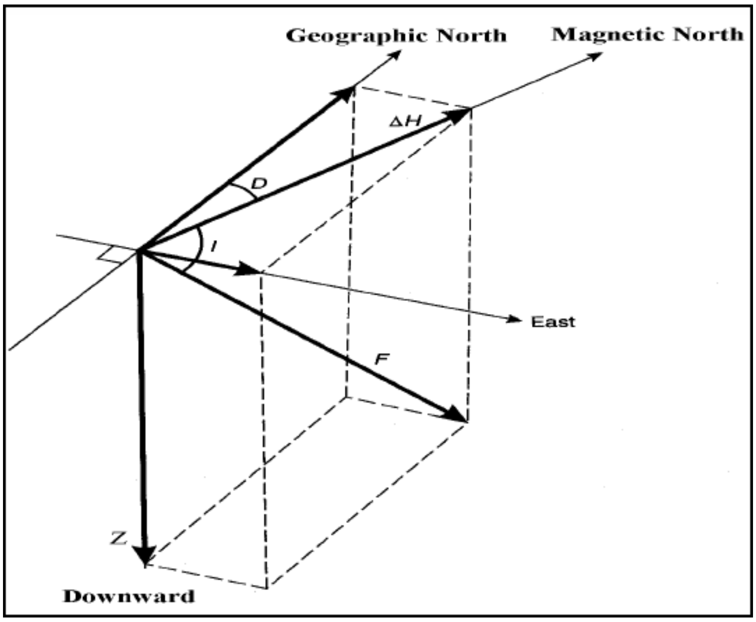

Figure 7: *The main magnetic field components.* ***F****-direction of earth's main magnetic field, D magnetic declination, I-magnetic inclination, H-Horizontal component of the main magnetic field (adapted from Reynolds, 1998).*

Magnetic Properties of Materials

The magnetic characteristics of rocks and minerals are a complex subject whose details are still under investigation. However, for most engineering and environmental applications, the magnetic characteristics are usually controlled by the content of magnetic minerals (mainly magnetite) in a rock and the type of metal (mainly iron) composing buried drums, cables and pipes.

The magnetic readings measured by a magnetometer are usually assumed to be caused by magnetization induced in a magnetizable material (those with a large magnetic susceptibility) by the earth's main magnetic field. This magnetization is not permanent and is lost when the external field is removed. In addition, most rocks and minerals have a permanent magnetization called remnant magnetization that is acquired by a variety of mechanisms (Telford et al., 1990) and is usually in a different direction and magnitude than the induced magnetization. In most cases, the magnitude of the remnant magnetization is small compared to the induced magnetization and can be ignored, although for detailed surveys (source anomalies less than 5 gammas) it can be important, requiring laboratory analyze to determine the remnant magnetization properties of the rock or soil samples.

Most engineering and environmental magnetic studies involve taking readings over soil, which in most situations has a low magnetic susceptibility and the interpreter will not have to be concerned with anomalies caused by magnetic susceptibility variations within the soil. However, the magnetic susceptibilities of a soil reflect their source rocks, as soils derived from mafic igneous rocks (e.g., basalts and gabbros) tend to have a high magnetite content (Sharma, 1997). Furthermore, magnetite is a heavy mineral, resistant to weathering, so it tends to accumulate in river deposits, beach sands and alluvial fans, and thus may create magnetic anomalies in areas of accumulation. In addition, highly organic soils often contain magnetite, a mineral with a high magnetic susceptibility and may cause localized magnetic anomalies.

Diamagnetism, Paramagnetism and Ferromagnetism

All atoms have a magnetic moment as a result of the orbital motion of electrons around the nucleus and the spin of the electrons. According to quantum theory, two electrons can exist in the same electron shell (or state) as long as they spin in opposite directions. The magnetic moments of two such electrons, called *pair electrons,* will cancel out. In the majority of substances, when there is no external applied magnetic field, the spin magnetic moments of adjacent atoms are distributed randomly so there is no overall magnetization. In a *diamagnetic* material, such as halite, all the electron shells are completely filled so there are no unpaired electrons. When an external magnetic field is applied, a magnetization is induced. The electrons orbit in such away so as to produce a magnetic field that opposes the applied field giving rise to a weak, negative susceptibility. Unpaired electrons in incomplete electron shells produce unbalanced spin magnetic moments and weak magnetic interactions between atoms in *paramagnetic* materials such as amphiboles, olivines, garnets and biotite. In an external applied field, the spin magnetic moments align themselves into the same direction, although this process is retarded by thermal agitation. The result is a weak positive susceptibility according to the Curie-Weiss Law. Paramagnetism is generally at least an order of magnitude stronger than diamagnetism. In *ferromagnetic* materials, the susceptibility is large but is dependent upon temperature and the strength of the applied magnetic field. The spin moments of unpaired electrons are coupled magnetically due to the very strong interaction between adjacent atoms and overlap of electron orbits. A small grain in which magnetic coupling occurs forms what is called a *single magnetic domain* and has dimensions of the order of micron. This gives rise to a strong .spontaneous magnetization. that can exist even when there is no external applied field. The magnetic coupling can be such that the magnetic moments are aligned either parallel or antiparallel.

Truly ferromagnetic materials occur only rarely in nature but include substances such as cobalt, nickel, and iron, all of which have parallel alignments. Ferromagnetism disappears when the temperature of the material is raised above the *Curie temperature* T_C , as inter-atomic magnetical coupling is severely restricted and the material thereafter exhibits paramagnetic behavior.

In *antiferromagnetic* material, for example hematite, the moments are aligned in an antiparallel manner. Although the magnetic fields of the oppositely oriented dipoles cancel each other out, crystal lattice defects result in a net residual moment or *parasitic (anti)-ferromagnetism.* In ferrimagnetic materials, of which magnetite, titanomagnetite and ilmenite are prime examples, the sub-lattices are unequal and antiparallel. This results in a net magnetization. Spontaneous magnetization and large susceptibilities are characteristics of ferrimagnetic materials, such as in the case of pyrrhotite. Although the temperature dependence of ferrimagnetic behavior is complex, ferrimagnetism disappears at temperatures above the Curie point. The majority of naturally occurring magnetic materials exhibit either ferrimagnetic or imperfectly antiferromagnetic characteristics.

Corrections to Magnetic data observations and Magnetic Noise

The observed magnetic readings obtained from a magnetic survey reflect the earth's total magnetic field including the earth's main field, diurnal variations and crustal magnetization sources. Two main corrections are applied to the data are diurnal variation and IGRG correction.

The Diurnal Variation

Variation of earth`s magnetic field with time, due to the rotation of the earth and with respect to the solar wind, which may last several hours to one day, is called diurnal variation (Riddihough, 1971).

A diurnal correction can be applied by reoccupying the same site at regular intervals (not more than an hour apart), producing a diurnal curve and adding or subtracting the appropriate correction to the acquired value.

Removal of the main earth`s magnetic field (DGRF)

Magnetic survey involves the measurements of the sum of magnetic field produced by both local and regional magnetic field. The regional magnetic field DGRF (Definite Geomagnetic Reference Field) often refers to as geomagnetic field needed to be subtracted from the acquired total magnetic field to obtain the magnetic field anomaly caused by the local source.

Magnetic Noise

Any noise or disturbance in the ground or its equipment that could produce a signal on the recorder is classified as a magnetic noise.In ground magnetometer surveys, it is always advisable to keep any magnetic objects (keys, penknives, some wristwatches iron belt, etc), which may cause magnetic noise, away from the sensor. It is also essential to keep the sensor away from obviously magnetic objects such as cars, metal sheds, power lines, metal pipes, electrified railway lines, walls made of mafic rocks, etc.

Analytic signal: Absolute analytic signal according to Roest et al. (1992) defined as the square root of the squared sum of the vertical and the horizontal derivatives of the magnetic field. $AS = \sqrt{\delta x . \delta x + \delta y \delta y + \delta z \delta z}$ Where $\delta x \; and \; \delta y$ are horizontal δz is vertical derivatives AS is the analytic signal.

REFERENCES

AGI, (2008). *Instruction Manual for Earth Imager 2D Version 2.2.8, in. Ed.: Texas, USA, Advance Geosciences Inc, pp 1-136.*

Anthony, E., (2005). *An introduction to ore geology. Geosciences text v.2, pp*

Asrat Asfaw., Barbey, P., Gleizes, G. (2001*). The Precambrian Geology of Ethiopia: a review. Africa Geosciences Review, 8: 271-288.*

Asrat Asfaw., Barbey, P., Ludden, J., Reisberg, L., Gleizes, G., Ayalew, D. (2004). *Petrology and isotope geochemistry of the Pan-African Negash pluton, Northern Ethiopia: Mafic-felsic magma interactions during construction of shallow-level calc-alkaline plutons. Journal of Petrology, 45: 1147-1179.*

Ayalew Teklewold., Bell, K., Moore, J. M., Parrish, R. R. (1990). *U-Pb and Rb-Sr geochronology of the Western Ethiopia Shield. Geol. Soc. Am. Bull., 102: pp 1309-1316.*

Ayalew Teklewold., Moore, J. M. (compilers) (1989). *Final Report of the Gore-Gambella Geotraverse, western Ethiopia.* International Development Research Centre (IDRC), Canada, 153pp.

Ayalew Teklewold., Peccerillo, A. (1998). *Petrology and geochemistry of the Gore-Gambella plutonic rocks: implications for magma genesis and the tectonic setting of the Pan- African Orogenic Belt of Western Ethiopia. Journal of African Earth Sciences, 27: 397-416.*

Boonchaisuk, S., Vachiratienchai, C., and Siripunvaraporn, W., (2008). *Two-Dimensional direct current (DC) resistivity inversion: Data space Occam`s approach: Physics of the Earth and Planetary Interiors, v. 168, pp 204-211.*

Daniels F. and Alberty R.A., (1966). *Physical Chemistry. John Wiley and Sons, Inc.*

Dey A. and Morrison H.F. 1979a. *Resistivity modelling for arbitrary shaped two-dimensional structures. Geophysical Prospecting **27**, 1020-1036.*

Dey A. and Morrison H.F., 1979b. *Resistivity modeling for arbitrarily shaped three-dimensional shaped structures. Geophysics* ***44****, 753-780.*

EL-Mining second year follow up report (May, 2010). Unpublished paper.

El –Mining third year follow up report (March, 2011). Unpublished paper.

Ethiopia scr-scribd (2011), *mining journal: a supplement of mining journal. Available at URL: www.scribd.com/doc/63931414/Ethiopia-scr. Date accessed Sep, 2011.*

Geological survey of Ethiopia. **(2000**). *Geology of the Gimbi area. Compiler Alemu, T. and Abebe, T.,Memoir 15,157p.*

Griffiths***, D. H.*** **&** **King*****, R. F. (*****1965).** *Applied geophysics for engineers and geologists.* King *Pergamon Press, Oxford.*

Groves, D.I., (1990). *Geological concepts in the exploration for large to giant late-orogenic (Mesothermal) gold deposits: The Archean greenstone experience. In: Mesothermal Gold Deposits: A Global Overview. Geol. Dept. (Key Centre). Univ. Ext., Univ. West. Aust. Publ. 27, pp 114–117.*

Kazmin, V., A. Shiferaw, M. Tefera, S.M. Berhe and S. Chewaka, (1979). Precambrian structure of Western Ethiopia. Ann.Geol. Surv. Egypt, pp 1-18.

Keller G.V. and Frischknecht F.C.,(1966). *Electrical methods in geophysical prospecting. Pergamon Press Inc., Oxford.*

Kirsch, R., (2006). *Groundwater Geophysics. A Tool for Hydrogeology.* Springer-Verlag Berlin Heidelberg, Germany.

Kula, C. Misra, (2000). Understanding mineral Deposits. University of Tennessee, Knoxville, U.S.A., pp 698-737.

MacLeod, I. N.,K. Jones, and T. F.Dai, (1993***)****. 3-D analytic signal in the interpretation of total magnetic field data at low magnetic latitudes. Exploration Geophysics, 24, pp 679–687).*

Macleod, I.N., Vierra, S. and Chaves, A. C., (1993). *Analytical signal and reduction to-the-pole in the interpretation of total magnetic field at low magnetic latitudes. Proceeding of the Third International Congress of the Brazilian Geophysical Society, November 1993.*

Maddalena, F., Salvatore, P., Solomon Tadesse, and Paolo, V., (2008). Epithermal gold occurrences in the lakes district of the main Ethiopian rift and tendaho (Afar rift): Discovery of a metallogenic province. Available at **http://*www.cprm.gov.br/33IGC/1351251.htm***. *Date accessed Oct 2011.*

.**Moore, J. M., Morgan, J., Tefera M, Teklay Mengisti., (1987**). *Geology of the Gore-Gambella Geotraverse, western Ethiopia. In Current Research in African Earth Sciences (edited by Matheis, G., Schandelmeier, H), 109-112. Balkema, Rotterdam/Boston.*

Pazdirek, O. and Blaha, V., 1996. Examples of resistivity imaging using ME-100 resistivity field acquisition system. EAGE 58th Conference and Technical Exhibition Extended Abstracts, Amsterdam.

Parasins, D.S., (1975). *Mining geophysics, 2nd ed. Elsevier scientific publishing company Amsterdam/ oxford/New York. PP 17-19.*

Reynolds, J.M., (1990). *An introduction to applied and environmental application of geophysics*. pp, 522-552.

Riddihough, R.P., (1971). Diurnal Corrections To Magnetic Surveys — An Assessment Of Errors, Geophysical Prospecting, v. 19, pp, 551-567.

Roest,W.R., Verhoef, J., and Pilkington, M., (1992). *Magnetic interpretation using the 3D-Analytic signal.*: Geophysics v. 57, p.116-125.

Sharma, P.V., (1997). *Environmental and engineering geophysics: Cambridge Univ. Press.*

Silvester P.P. and Ferrari R.L., 1990. *Finite elements for electrical engineers 2nd. ed., Cambridge University Press.*

Solomon Tadesse, (2009). *Mineral resources potential of Ethiopia*, Addis Ababa University press, pp 5-7, 34-35, 37-55**.**

Sumner, J.S., (1976). *Principles of induced polarization for geophysical exploration*: Elsevier scientific publishing company, pp 277.

Tatsch, J.H., (1975). *Gold deposits. USA press.*

Tefera Mengistu., Berhe, S. (compilers) (1979); *The Geological Map of the Gore Map Sheet. Ethiopian Institute of Geological Surveys, Addis Ababa, Ethiopia.*

Telford, W.M., Geldart, L.P., and Sheriff, R.E., (1990), *Applied geophysics, second edition. Cambridge University Press.*

Telford, W.M, (1996). Applied geophysics.Cambridge University Press.

Van Voorhis, G.D. Nelson, P.H. and Drake, T.L., (1973). *Complex resistivity spectra of porphyry copper mineralization. Geophysics, **38**, pp 49-60.*

Westerhof, A. (1999). *Area selection, terrain analysis and ore deposit modelling. ITC, Branch of Exploration and Engineering Geosciences Kanaalweg 3; 2628EB Delft, The Netherlands.*

Wolde Begashaw., Gore-Gambella Geotraverse Team, 1996; *Tonalite-trondjemite granite gneiss by partial melting of newly under plated basaltic crust: an example from the Neoproterozoic Birbir Magmatic arc, western Ethiopia. Precambrian Research, 76, pp 3-14.*

Zonge Abstract (2011), *Geophysical prospecting methods*. Available at URL: www.zonge.com/HTM_Papers/GeophysicalProspectingMethods.html.Date accessed Sep, 2011.

Declaration

This thesis is my original and has not been presented for the degree/masters in any other university, and that all the sources of materials used for the thesis have been duly acknowledged.

Fantahun Gebrie Teshome

Signature_____________ Date ___________________________

Dr. Shimeles Fisseha (Advisor)

Signature _______________ Date______________________

November 2011

Addis Ababa

ETHIOPIA